FABRICATION AND CHARACTERIZATION OF PHYTOCHEMICALS INCORPORATED ECM-POLYMER FUNCTIONAL FILMS FOR CHRONIC WOUND HEALING

A THESIS SUBMITTED IN PARTIAL FULFILLMENT

OF THE REQUIREMENTS FOR THE DEGREE OF

Master of Technology

In

Biotechnology

By

MISS SOMYA ASTHANA

212BM2007

Under The Supervision of

PROF. SIRSENDU SEKHAR RAY

and

Co-supervision of

DR. A. G. SAMAL

Department of Biotechnology & Medical Engineering

National Institute of Technology Rourkela-769008, Orissa, India

2014

Dr. (Prof.) Sirsendu Sekhar Ray
Assistant Professor
Department of Biotechnology & Medical Engineering
National Institute of Technology, Rourkela, Orissa, India

Certificate

This is to certify that thesis entitled "**Fabrication and characterization of phytochemicals incorporated ECM-polymer functional films for wound healing**" by **Miss Somya Asthana**, submitted to the National Institute of Technology, Rourkela for the Degree of Master of Technology is a record of bonafide research work, carried out by her in the Department of Biotechnology and Medical Engineering under my supervision and guidance. To the best of my knowledge, the matter embodied in the thesis has not been submitted to any other University/ Institute for the award of any Degree or Diploma.

Dr. (Prof.) Sirsendu Sekhar Ray

Assistant Professor

Department of Biotechnology and Medical Engineering

National Institute of Technology, Rourkela

ACKNOWLEDGEMENT

The project is incomplete without the appreciation to those who played an important role in the completion of my project. With overwhelming and embedded feeling of gratitude, I would like to express my sincere appreciation to all those who directly or indirectly contributed towards completion of this project. I would like to express my deep sense of heartfelt gratitude and regards to my supervisor **Dr. Sirsendu Sekhar Ray**, Department of Biotechnology and Medical Engineering for giving me an opportunity to do the project work and keeping faith on me for carrying out my work.

I consider it a privilege to express my gratefulness to **Dr. Ajit Samal**, Super Speciality Hospital, Rourkela, for being my co – supervisor and for providing constant support to me. I am deeply indebted to **Dr. Indranil Banerjee and Dr. Kunal Pal**, and **Dr. Krishna Pramanik**, Department of Biotechnology and Medical Engineering, National Institute of Technology Rourkela for the valuable guidance, help and suggestions during the project work.

Further, I would like to express my thankfulness to **Mr. Tarun Agarwal, Mr. Susanta Basuri, Mr. Mohit Gangwar, Mr. Rik Dhar** and **Miss Priyanka Goyal** for their constant support and advice in my project work. I sincerely thank all my faculty members for their blessings.

Finally, I am grateful to my parents **Dr. Rakesh Asthana** and **Mrs. Mamta Asthana,** family members and friends for their endurance, love, wishes and support, which helped me in completion of my work. Above all, I thank **GOD** who showered his blessings upon us.

(**Somya Asthana**)

CONTENTS

ABSTRACT

Chronic wounds are such wounds which do not heal through normal physiological healing process. Different bandages and medicines have been tried to heal such wounds but these are very recalcitrant to get healed. Millions of people are being affected by these and hence need special attention. Major reasons for pathogenesis of chronic wounds mainly include insufficient and disorganized extracellular matrix (ECM), insufficient angiogenesis, adipogenesis, and some ulcers caused by chronic infections, that all together lead to chronic inflammations and the persistence of these wounds. Therefore, in my study, I targeted all the above mentioned causatives of chronic ulcers by the preparation of ECM based composite scaffolds which were then characterized through swelling, water vapor permeability, biodegradability, in – vitro cytotoxicity, XRD, FTIR, etc. Phytochemicals being famous for their medicinal values have been used since ages. Therefore, Curcumin, a well known phytochemical was incorporated in the prepared film to study the drug release kinetics. The effect of the phytochemicals was studied over angiogenesis, adipogenesis and over special category of ulcers through *in silico* analysis. The selected phytochemicals were also extracted as a crude extract through the soxhlet method, which were then screened through biochemical tests. Concentration of these phytochemicals was also optimized for the stem cell proliferation and was found to be compatible with them.

Keywords- Chronic inflammations, angiogenesis, extracellular matrix, Polymer, Proliferation, Phytochemicals

LIST OF TABLES:

LIST OF FIGURES:

INTRODUCTION

Skin, being the first barrier in the body defense plays a very important role in preventing the body from various infections, diseases and disorders. Any injury to this protective layer, that is, skin lead to different types of wounds which depend upon the degree of the injury caused. Healing of such injuries is a natural process which begins soon after the injury and completely recovers the injured or wounded tissue. This is a general phenomenon which includes various interlinked and overlapping phases: Hemostasis and inflammation, Re-epithelialization and Remodeling.

Hemostasis and Inflammation stage includes the initial breakage of the epithelial tissue lining which activates the clotting factors. Fibrinogen begins the clotting of blood through the fibrin formation. Inflammation starts within 24 hours of hemostasis and can be extended upto 49-72 hours. This phase causes dilation of the blood vessels, thus initiating the infiltration of the inflammatory cells. Platelets, itself being released from thrombus, release the growth factors like Platelet derived growth factor (PDGF) and Transforming growth factor – β (TGF-β). The above mentioned infiltration of inflammatory cells includes the chemotactic movement and the proliferation of the macrophages and the neutrophils. Both, neutrophils and macrophages eat away the debris of the necrotic tissue[1]. Unlike neutrophils, the macrophages release certain rowth factors and cytokines such as interleukins (IL-1, IL-6, and IL-8), PDGF, TGF-β, Insulin growth factor (IGF), Vascular Endothelial Growth Factor (VEGF), and Fibroblast Growth Factor (FGF), which inturn helps in the revival and proliferation of the cells near the wound site like endothelial cells and the fibroblast cells along with more macrophages[2].

Proliferative stage completely rotates around the fibroblast cells which produce collagen, not only to provide structural support but also replaces the matrix formed from the composite of fibrin and fibronectin. This fibroblasts proliferation continues with the formation of blood vessels, commonly known as angiogenesis [3]. Apart from the major role played by the fibroblast cells, epithelialization of the keratinocytes over the wound also occur during this phase.

Remodeling stage begins with the advancement of the synthesis of collagen and the degradation of the same. Fibroblasts producing collagen crosslink it, thus increasing the wound toughness

accompanied by the contraction of the wounds. This takes two to three weeks or may be upto 2 years, depending upon the type of wound.

The wounds can be categorized into: Open and closed wounds as per the amount of exposure of the wounds to the environment. The wounds can also be classified as Acute and chronic wounds. Acute wounds are such wounds which get healed up within a time of repair whereas the chronic wounds are those which are hard to heal wounds and do not follow the normal physiological process of healing. This improper healing in chronic wounds inturn leads to chronic inflammations causing the development of various ulcers like diabetic foot ulcer, pressure ulcers and venous ulcers[4].

Chronic wounds like those mentioned above results from various factors due to the reason that these factors delay the wound closure and thus the healing of the wounds. The factors affecting wounds include: Infections, Moisture in the wound site, Age, Stress, Obesity, disorders like Diabetes, non steroidal anti – inflammatory drugs, smoking and Alcohol intake. These major criterions decide how early or how late the wounds get healed.

The major cause of such hard to heal wounds is:

- Chronic Inflammation
- Insufficient Extracellular Matrix (ECM)
- Insufficient Angiogenesis
- Insufficient Adipogenesis
- Special category of ulcers.

In wounds, the immune system responds back to cause inflammation in the body but sometimes like those in chronic wounds, the inflammation not only kill microbes but damage tissue as well. When the inflammation goes on for long durations, it causes infiltration of macrophages, monocytes, lymphocytes and plasma cells, instead of neutrophils. Due to the interaction of the inflammatory cells for a longer period of time, the tissue gets damaged by these cells [5].

ECM plays a very important role in tissue regeneration and wound healing. It provides communication between the cells causing them to adhere, proliferate and differentiate over the surface of ECM. Insufficient ECM at the wound delays the healing process as it provides the

structure and adhesion to the cells and the growth factors embedded in it. Growth factors rely over the ECM for their activity and in the absence of ECM, the repairing process of the injured tissue gets disturbed [6]. Therefore the external addition of ECM can be a preferable option as in chronic wounds, the high level of inflammatory cells can inturn release proteases which degrade the ECM components and growth factors which is crucial for healing.

Like ECM, Angiogenesis is a crucial factor in Tissue Engineering. Insufficient angiogenesis can cause hypoxia to occur which is unfavorable for the healing of wounds. The reason behind is known to be the inflammatory responses which delays the healing process due to release of oxygen free radicals. The overproduction of proteases from the inflammatory cells promotes the tissue necrosis and delays the normal healing and repair process.

It has been recently found that the adipocytes interact or communicate with the fibroblast cells and repopulate during the second phase, that is, proliferative phase of the wound healing process. Adipogenesis is the process through which the adipocytes proliferate and migrate from the non – injured site to the injured one, thus increasing their population. Thus, insufficient adipogenesis can lead to improper proliferation and interaction of adipocytes with the fibroblasts [7].

Beside these causes, there are some distinct types of ulcers which come in the category of the chronic wounds. These include: tubercular ulcers, leishmanial ulcers, and ulcers due to the severe effects of cancer and AIDS. These are some of the major cause of the persisting wounds.

Many treatments have been applied for the cure of the above mentioned problems in chronic wounds and in early closure and healing of the same. The use of biocompatible matrices has been recently produced and is used for this purpose. Some of them are Epidermal Autografts, Apligraf, and Dermagrafts [8-9]. Many hydrogels, foams, negative pressure topical dressings, and hydrocolloids are there which are recently been used [10-14]. Other than these, acellular matrices are also accepted for their applications in chronic wounds. These include not only human tissue (allograft), animal based tissue (xenograft), but also the scaffolds with collagen in it.

In this study, all the five factors responsible for the chronic wounds have been dealt. For the study of chronic inflammation and insufficient ECM, polymer – ECM based films have been developed and characterized along with drug release kinetics using Curcumin which plays an

important role in treatment of chronic inflammation. The problem of insufficient angiogenesis is dealt using phytochemicals, known for their angiogenic properties through *in-silico* as well as through experimental methods. Similarly, insufficient adipogenesis is dealt through the study of the effect of the phytochemicals over cellular proliferation through in-silico as well as in-vitro analysis. The special category of ulcers was also studied using the multiple medicinal properties of an herbal plant Asparagus racemosus through in-silico analysis.

I. INSUFFICIENT EXTRACELLULAR MATRIX

Chronic wounds affect millions of people exposing them to pain and reduced quality of life. These can be majorly due to diabetes, venous leg ulcers or application of pressure for prolonged period of time due to limited mobility. The progression of such wounds through normal physiological healing process [15] often fails due to aberrant prolongation of the inflammatory phase [16]. It is observed that these wounds are consequences of abnormal physiological conditions such as insufficient blood supply and excessive degradation of extracellular matrix (ECM) leading to structural and functional impairment [17] of underlying tissue and self-repair is generally troublesome [18]. The treatment mainly involves regeneration or replacement of damaged or missing tissue. Many of the researchers have found success in their attempts to engineer the damaged tissue [19] by using natural materials as substitutes [20-21]. Many such skin substitutes, that mimic human ECM, have been developed and commercialized [22]. Those materials have been mainly constituted of ECM derived from bovine or porcine dermal, submucosal or urinary bladder tissue [23-24]. The beneficial effects of these xenogenic products are because of their external supplementations of ECM and growth factors at the wound site. At the injury site, these xenogenic ECM provide structural and functional support for cells and binds to various growth factors, thus creating pool of active molecules and enhancing the cell proliferation and migration, thus mobilizing the injury during wound healing. It is also important to mention that the native ECM is also known to guide the immune cells. Thus, direct use of ECM could modulate the aberrant inflammatory phase and may play a role in better and efficient healing of chronic wounds [25].

Though, omentum is known as the ‘policeman of the abdomen’ and is having very high proportion of ECM and growth factors, the omental ECM has never been utilized for the wound healing purposes. Supplementing the above facts, the greater omentum has been recently engaged for the isolation of ECM due to its rich vascular inventories and high level of angiogenic properties to support and provide higher amount of growth factors, thus enhancing hemostasis and preventing immune rejection of the implant [26-31].

It is often observed that use of only ECM as scaffold undergoes faster degradation in presence of proteases which are usually released by inflammatory cells in high concentration during chronic wounds [32-33]. For this purpose, use of biopolymer composites has gained a great importance [32, 34]. In this regard, chitosan deserves a special attention due its wound healing capabilities [35]. Chitosan is a natural polysaccharide composed of monomers β-1, 4 glucosamine (2-amino-2-deoxy-β-D-glucose) and N-acetylglucosamine. It is considered to be very promising material due to its biocompatibility, biodegradability, low immunogenic and antimicrobial properties [36-37]. As the wound bandages, chitosan itself binds with the red blood cells and initiate rapid clotting. In addition, it also preserves exudative wounds by restraining it from getting dried and contaminated, so as to promote a better condition for healing [37]. In recent years, chitosan has been explored extensively as wound dressings for wound healing and tissue engineering applications [38-40]. Chitosan has also been used to prepare hydrogels as wound dressings [41], gels for wound burns [42], sponge, fiber [43] as well as composite scaffolds along with collagen [44-45], silk fibroin and alginate dialdehyde [46], gelatin [47-49], hydroxyapatite [50], heparin [51] lignin [52] as well as methoxy poly(ethylene glycol) [53] to speed up the healing process.

Alginate is a naturally existing hydrophilic polysaccharide which is generally isolated from seaweeds. It is a polymer of 1-4 β – D – mannuronic acid (M) and α – L – guluronic acid (G) monomers. Alginate is widely known for its biocompatible, biodegradable, non – antigenic and chelating abilities, which makes it a suitable candidate in tissue engineering and biomedical applications [54-55].

Besides being non – toxic, Alginate is known to have good water absorptivity, optimal moisture and air transmission rate and antiseptic properties. Especially for the exudative wounds, Alginate based wound dressings are already in market. These include sponges, hydrogels, electrospun mats that enhance the gel forming as well as hemostatic ability of the dressing [56-57].

Alginate has also been complexed with chitosan and fibrin so as to prepare and characterize the composite sheets which can be used as a wound dressing**.** Alginate based gels are also recognized to promote healing by preventing the wound bed from getting dried. Recently, it was found that alginate based dressings can increase the healing rate by stimulating monocytes to release cytokines as tumor necrosis factor – α and interleukin – 6.Apart from this, the alginate based dressing provide an anti – microbial environment for a better wound repair and prevent colonization of micro – organisms that can cause infection and delay in healing [58].

It is important to mention that use of ECM – Chitosan and ECM – Alginate composite may combine the advantageous properties of the individual components that may provide better cell adhesion and growth, thus enhancing the rate of tissue healing. Therefore, in the current study, we prepared porcine omental derived ECM – Chitosan composite films and characterized them for its application in chronic wound healing.

1.1 MATERIALS AND METHODS

Materials:

Chitosan, Dulbecco's Minimal Essential Media (DMEM), Dulbecco's Phosphate Buffer Saline (DPBS), Trypsin-EDTA solution, Fetal Bovine Serum, Antibiotic-Antimycotic solution, MTT assay kit and Nutrient Broth were purchased from Himedia, Mumbai, India. Sodium Alginate was purchased from S.D.Fine – Chem. Ltd. The gluteraldehyde (25% aqueous solution) was procured from LOBA Chemie, Mumbai, India. Collagenase and Lysozyme enzyme was bought from MP Biomedical and Otto Chemie, Mumbai respectively. The MG63 cell line was procured from NCCS, Pune. All other chemicals used were of analytical grade and were obtained locally.

Methods:

1.1.1 Decellularization and solubilization of Adipose Tissue:

Pig omentum tissue was obtained from the slaughter house, Malegam, Rourkela under the sterile conditions. The tissue was washed in phosphate buffer saline (pH 7.4) thoroughly to remove any blood components. The double volume of phosphate buffer saline was added to the washed tissue and was homogenized in blender for 5 min with pulsation of 30 seconds. A thick paste of the homogenized tissue was then centrifuged at 8000 rpm for 10 min. The blended tissue got separated into three layers – supernatant, middle layer and pellet/debris. The supernatant consists of fat or oil due to defatting of omentum which was then discarded. After discarding the supernatant, the remaining was subjected to repeated freeze thawing (-21^0C then 37^0C). Thereafter, the samples were centrifuged again until no oil layer was found. The middle layer which is mostly tissue now consists of extracellular matrix was collected for subsequent processing. The tissue was then washed with distilled water, 0.2% DNase and 0.5% SDS at 37°C for 1 day [59]. The decellularized tissue was then solubilized in 0.5 M acetic acid solution under

continuous stirring for 48 hours. The solution was then filtered through muslin cloth and centrifuged again at 8000 rpm for 10 min to get pure ECM. The ECM was then stored at 4°C for further use.

1.1.2. Preparation of polymer-ECM composite films:

2% chitosan (Degree of deacetylation > 75%) solution was prepared in 0.5 M acetic acid solution under stirring condition. 2% alginate solution was prepared in distilled water. For which, 2gm sodium alginate powder was slowly added to distilled water under stirring condition. A homogenous solution was prepared through a continuous and overnight stirring. On other hand, the ECM pellet obtained after decellularization of omentum tissue, was lyophilized to remove the water content from ECM pellet. Thereafter, lyophilized ECM was dissolved in 0.5M acetic acid solution to get a final concentration of 50 mg/ml, 100 mg/ml and 150 mg/ml. Thereafter, Chitosan and ECM solution (all concentrations), were mixed in 6:4 (w/w) ratio under stirring conditions followed by degassing. The chitosan-ECM composite films were prepared using Casting/ Solvent evaporation Technique as described by Maryam Koucha et al. [60]. 30 gm each of prepared Chitosan-ECM solutions were poured in the 90mm petri dish and dried for 48 hours in the vacuum oven (Q5247, Navyug, India) at 37°C. The dried composite films were removed from petri dish using 2N sodium hydroxide treatment for 30 minutes. Thereafter, the films were peeled out, washed 3-4 times with distilled water and kept for drying at 37°C for about 24 hours [61].

1.1.3. Characterizations of polymer-ECM composite films:

1.1.3.1. Thickness of the films:

The thickness of the films was measured using digital vernier caliper (Traceable® Digital Calipers 6in, Fischer Scientific). The thickness of each film was measured at ten different locations and was reported as a mean of all the measurements.

1.1.3.2. Swelling Test:

Polymer-ECM composite films of 1x1 cm^2 were initially cross-linked using 20% gluteraldehyde solution for about 12 hours which were then weighed after drying (W_d). The films were then

immersed in phosphate buffered saline PBS (pH 7.4) ant kept at 37°C. The films were removed from PBS, after a regular interval of time (5, 10, 15, 30, 60, 90 and 120 min). Thereafter, excess of PBS was blotted off from the films using filter paper (Sartorium Stedim Biotech grade) and wet weight of the films (W_t) were recorded at the above mentioned time intervals [62]. The experiment was performed in triplicates. The % swelling was calculated which is defined as the ratio of the weight increase ($W_t - W_d$) to the initial dry weight (W_d).

$$\textbf{Swelling ratio (\%)} = [(W_t - W_d) / W_d] \%$$

Where,

W_t = Wet weight of films

W_d = Dry weight of films

1.1.3.3. Moisture Absorption Test:

The films of 1x1 cm^2 size were completely dried in the Vacuum drying oven (Labtech) for 24 hrs and then taken in dessicator at 84% humidity by saturated solution of KCl for 12 hours. The final weight of the sample films was noted. The percentage of moisture absorbed from the environment in the standard conditions, was calculated:

$$\textbf{Percentage moisture absorbed (\%)} = [(W_f - W_i) / W_i] \%$$

Where,

W_i = Initial weight of the films

W_f = Weight (final) of the films after drying

1.1.3.4. Water Vapor Transmission Test:

Water vapor transmission or permeability of the Polymer-ECM composite film was evaluated using the water method (ASTME 96 standardized method) [63]. According to this method, the sample films were kept completely adhered on to the top of the cylindrical glass tubes (volume = 71.42 cm^3) using a Teflon tape (P.T.F.E Thread Seal Tape) (Figure 1).

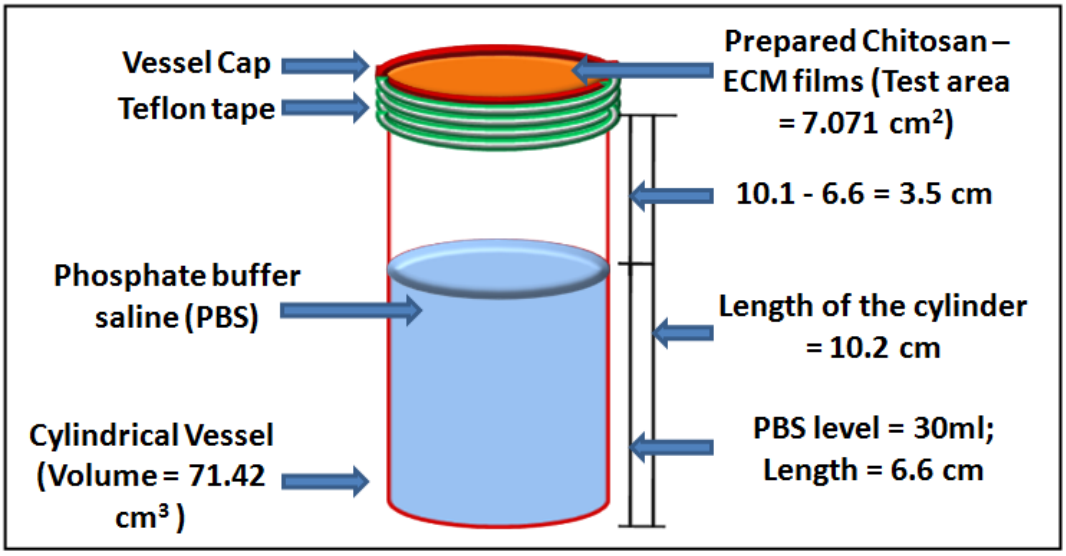

Figure 1. Set up for the water vapor permeability test

Each tube was initially filled with pre-weighed (30 ml) PBS. The initial weight and height of the water (from base) was recorded and then the tubes were kept at 37°C. The readings were taken daily for about more than two weeks. The transmission of water vapor through the chitosan-ECM composite films was calculated using equation:

Water Vapor Transmission rate (g/day-m^2) = [(Change in weight)/ (Time (days)] x Test area)

1.1.3.5. Biodegradation Test:

The films of 1x1 cm^2 size were taken in a 12 well plate and dry weight of the films was noted. An enzyme cocktail of Lysozyme-Collagenase in PBS (pH 7.4) was prepared under aseptic conditions (1/10th of total volume of Lysozyme (10,000 U/ml) - Collagenase (10 U/ml) solution was taken). 1 ml of prepared enzyme cocktail was added to the films under aseptic conditions [64] and the weight of films was recorded at definite interval of 15, 30, 60,120, 180, 240, 300, 360,720 and 1440 min. The percentage weight loss was calculated using formula:

$$\% \text{ Weight loss} = [(W_i - W_f)/ W_i] \%$$

Where,

W_i = Initial Weight of the film,

W_f = Final Weight of the film

1.1.3.6. Hemocompatibility Test:

The hemocompatibility of polymer – ECM composite films were analyzed. The leachant preparation was carried out by immersing dried films (cut into 1x1 cm^2) placed in a dialysis membrane in 10 ml of PBS (pH 7.4) under stirring condition of 60 rpm at 37°C for overnight. For Hemocompatibility studies, fresh goat blood was taken and diluted in 1:1 ratio with 0.9% normal saline. 0.5ml of leachant was added in blood suspension (9ml normal saline + 0.5 ml diluted blood) followed by the sample incubation at 37°C for 1 hour. Thereafter, the samples were centrifuged at 3500 rpm for 5 minutes and the supernatant was analyzed for the optical density at 545nm. The positive and negative controls were prepared by adding 0.1N HCl and normal saline respectively instead of leachant samples [65]. The percentage of haemolysis was measured by the following equation:

% Haemolysis = [(Test sample – Negative Control) / (Positive Control – Negative control)] x 100

1.1.3.7. *In vitro* Cytotoxicity Test:

The biocompatibility studies were performed using MG63 cell line, procured from NCCS, Pune. The cell line was maintained in Dulbecco's Modified Eagle Medium (DMEM) with 10% Fetal Bovine Serum (FBS) in incubator at 37°C, 5% CO_2 and 95% humidity. The cells were harvested using 0.25% Trypsin-EDTA solution and the viable cell density was analyzed using Trypan Blue dye exclusion test. Thereafter, the cells were seeded at a concentration of (1×10^5) cells/ml on sterilized film samples. Prior to seeding of cells, the films were subjected to UV and ethanol sterilization. The culture plate was incubated for next 24 hours. Further, the cell viability was accessed using MTT Assay [66-67]. The biocompatibility studies were done in quadruplet for each sample and the data was reported as relative proliferation index.

1.1.3.8. Fourier Transform Infrared Spectroscopy:

The polymer – ECM composite films (including the control samples of films) were examined for spectroscopic analysis using FTIR spectroscopy ATR mode (Shimadzu/IR prestige 21). The samples were analyzed keeping air as the reference. Scanning was done at the range of 4000 cm^{-1} to 500 cm^{-1} with a resolution of 4 cm^{-1}.

1.1.3.9 X- Ray Diffraction:

The X-ray diffraction pattern of polymer – ECM composite films was analyzed using X-ray diffractometer (PW3040, XRD-PANalytical, Philips, Holland). Cu-Kα radiation with wavelength 0.154 nm was used as a source. The instrument was operated at 30 KV and 20mA. Scanning of the samples was done at 5° - 50° (2θ) with a rate of 2° (2θ) /min. The analysis was performed at the room temperature.

1.1.4 Statistical Analysis:

Each experiment was performed in triplicates. All the results were mentioned as the average (mean) ± S.D. Statistical analysis of all the quantitative data was done using one – way ANOVA through IBM SPSS Statistics 20.0. The results of all the samples were compared at 95% of confidence level. The results with p – value equal or less than 0.05 were considered to be statistically significant.

1.2. RESULTS AND DISCUSSIONS

1.2.1. Film Preparation:

For the preparation of chitosan – ECM composite films (Figure 2), acetic acid was preferred for solubilization of ECM as it was found to preserve the helical structure of collagen. Thereafter, the films were prepared using Casting/ Solvent technique. The films were dried at 37°C for 48 hours, thus forming thin films with sufficient mechanical strength to be used as wound healing bandages.

Figure 2. Chitosan – Extracellular matrix and Alginate – Extracellular matrix composite films

1.2.2. Characterizations of film:

1.2.2.1. Film Thickness:

The thickness becomes an important criterion of characterization for the films to be used for wound healing applications. It governs many of properties including water vapor permeability, moisture absorption, tensile strength and biodegradation. Thickness of all the polymer-ECM composite films was found to be significantly higher in comparison to chitosan control (Table 1) ($p < 0.05$). This could probably due to the higher ECM concentration in the composite films. However, it is interesting to mention that the increase in ECM concentration in the composite films did not contribute significantly in variations of film thickness. This may possible be due to insignificant difference in viscosity of ECM solution among all the three concentrations.

1.2.2.2. Swelling Analysis:

The swelling kinetics of a film is crucial determinant of its degradation kinetics and release kinetics. The swelling analysis reflects the affinity of the films towards water which directly corresponds to its hydrophilicity. For wound healing applications, hydrophilicity of the system determines its interaction with the tissue and aids to migrations and proliferation of cells subsequently leading to greater rate of wound closure. Also for exudative wounds, the films with better absorbing capacity are required which help in keeping the wound bed moist and exudate free. In our study, the swelling of the chitosan-ECM composite films as well as the alginate – ECM composite films were found to be significantly higher in comparison to chitosan as well as

alginate control ($p < 0.05$) (Figure 3, Table 1). It was observed that the increase in ECM concentration increased the water retention capability of the composite films. This could possibly due to increase in hydrophilicity of the composite films with the addition of ECM. However, an insignificant difference in swelling was observed between CE100 and CE150. This may be due to higher interaction between ECM fibers or ECM-chitosan backbone, which may restrict the number of free functional groups available to interact with water molecules. Similarly for alginate, there is a significant difference between the alginate control and the one with ECM.

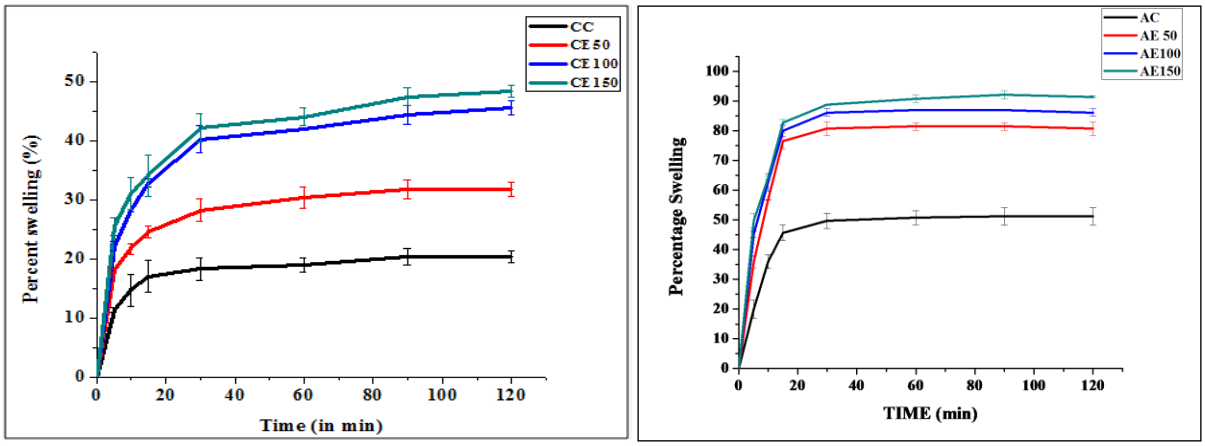

Figure 3. Swelling test of Chitosan – Extracellular matrix and Alginate – Extracellular matrix composite films

Table 1: Thickness, Percentage Swelling and Moisture absorption of ECM – Chitosan film samples

SAMPLE	Thickness ± Std Dev (mm)	% Swelling ± Std Dev (%)	% Moisture Absorbed (± Std Dev)
Chitosan Control (CC)	0.050 ± 0.01	20.325 ± 0.94	14.080 ± 1.03
Chitosan – ECM (50 mg/ ml) (CE50)	0.080 ± 0.01	31.826 ± 1.14	15.738 ± 2.18
Chitosan – ECM (100 mg/ ml) (CE100)	0.089 ± 0.01	47.198 ± 1.25	25.579 ± 1.82
Chitosan – ECM (150 mg/ ml) (CE150)	0.090 ± 0.01	48.464 ± 1.08	28.086 ± 2.26

Table 2: Thickness, Percentage Swelling and Moisture absorption of ECM – Alginate film samples

SAMPLE	Thickness ± Std Dev (mm)	% Swelling ± Std Dev (%)	% Moisture Absorbed (± Std Dev)
Alginate Control (AC)	0.061 ± 0.01	51.196 ± 0.94	15.749 ± 0.50
Alginate – ECM (50 mg/ ml) (AE50)	0.075 ± 0.01	80.729 ± 0.94	38.782 ± 1.31
Alginate – ECM (100 mg/ ml) (AE100)	0.078 ± 0.01	86.141 ± 0.94	42.631 ± 1.07
Alginate – ECM (150 mg/ ml) (AE150)	0.080 ± 0.01	91.403 ± 0.94	44.067 ± 2.02

1.2.2.3. Moisture Absorption Test:

Moisture absorption test is carried out to analyze the ability of the films to absorb moisture from the environment. It is generally seen that the presence of moisture accelerates the wound healing process. Thus, it becomes an essential selection criterion for selection of films suitable for wound healing applications. Both chitosan-ECM and alginate – ECM composite films demonstrated a higher degree of moisture absorption in comparison to chitosan and alginate control respectively ($p < 0.05$), under standard conditions of saturated solution of KCl. It is important to mention that with an increase in ECM concentration in the formulation, the moisture absorption ability of the films also increased (Table 1). However, increase in ECM concentration, results into low porosity of the films but increases the hydrophilicity drastically which may aid to better moisture absorption ability of CE150 in comparison to rest of the formulations. Similarly, decrease in porosity and increase in compactness results into lower chances of evaporation of absorbed moisture back into the environment.

1.2.2.4. Water Vapor Transmission Test:

According to the standards of ASTME, water vapor transmission rate or water vapor permeability refers to the flow of water vapor per unit time through a unit area of the body, under specific conditions of humidity and temperature. It is important to mention that the loss of water

vapour from the intact skin is 240-1920g/m^2/24 hours, while it rises to 4800g/m^2/24 hours in case of open wound [68]. As discussed above, wound healing is faster in the presence of moisture than in case of dry environment. Thus, ability of film to permeate water vapour becomes an essential criterion for their selection. The films may find variable applications depending upon their water permeability. A film with low water permeability could be effectively be used in low exudative wounds while a film with high water vapour permeability could be used for high exudative wounds. For polymer-ECM composite films, water vapour permeability test was carried out as per the protocol described in [63] and the data was recorded for 16 days. The variation in the water vapor transmission rate was found as statistically significant between the composites and control films ($p < 0.05$) (Table 3 and Table 4). In a wider view, as the ECM concentration was increasing, the transmission of water vapor was found to be decreasing. This can be due to the fact that ECM being hydrophilic and binds water molecule. Also, increase in ECM concentration decreases the porosity of films which may contribute to lower water vapour transmission.

Table 3: Water vapor transmission rate and percentage hemolysis of the Chitosan – ECM composite films

SAMPLE	**Water Vapor transmission rate ± Std Dev (g/day.m^2)**	**% Hemolysis ± Std Dev (%)**
Chitosan Control (CC)	2.799 ± 1.20	3.514± 0.14
Chitosan – ECM (50 mg/ ml) (CE50)	2.539 ± 0.58	2.882±0.26
Chitosan – ECM (100 mg/ ml) (CE100)	2.401 ± 0.26	2.792±0.87
Chitosan – ECM (150 mg/ ml) (CE150)	2.349 ± 1.19	2.072±0.48

Table 4: Water vapor transmission rate and percentage hemolysis of the Alginate – ECM composite films

SAMPLE	**Water Vapor transmission rate ± Std Dev (g/day.m^2)**	**% Hemolysis ± Std Dev (%)**

Alginate Control (AC)	3.821 ± 0.46	1.930 ± 0.24
Alginate – ECM (50 mg/ ml) (AE50)	3.529 ± 0.63	1.124 ± 0.99
Alginate – ECM (100 mg/ ml) (AE100)	3.103 ± 0.92	0.414 ± 0.83
Alginate – ECM (150 mg/ ml) (AE150)	2.898 ± 1.23	0.011 ± 0.75

1.2.2.5 Biodegradation Study:

The degradation profile of the films/bandages to be used for wound healing is of great importance. Once the films are applied onto the wound, they come in contact with variety of enzymes including Matrix Metalloproteinase's. It is also important to mention that, apart from enzymes from human source; the enzymes from microbes present in the environment also interact with the matrix and degrade it. Thus, it is important to characterize the degradation profile of the films before use. In our analysis, films were treated with Lysozyme-Collagenase solution in PBS with lysozyme and collagenase in concentration of 10,000 U/ml and 10 U/ml respectively, and the weight of the film sample was weighed at regular interval (Figure 4). Initially, the weight of the sample increased, due to the dilation in the samples due to the swelling. The differences in the degradation profile of the formulated films were found to be insignificant.

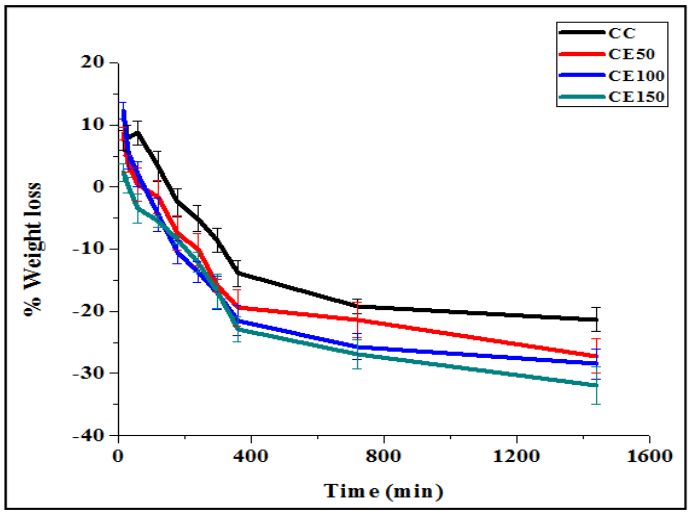

Figure 4. Biodegradability Test of Chitosan – Extracellular matrix composite films

The Alginate – ECM composite films got disintegrated within an hour. This may be due to the reason that the films were not crosslinked. The swelling that was observed in the biodegradation study was not upto the extent as observed in the swelling study because of the simultaneous biodegradation of the films in the presence of the enzymes. This was supported with the further fact that the control samples which were taken only in PBS, the increase in weight continued upto 2 hours, before decrease in the weight starts because of disintegration and degradation.

1.2.2.6. Hemocompatibility Test:

Hemocompatibility assay is one the essential criteria in analyzing the compatibility of the polymer blends. Autian suggested that the hemocompatibility of the polymer depends on the extent of hemolysis. Percentage hemolysis less than 5% indicate high degree of hemocompatibility, whereas equal or more than 5% indicate moderate or least hemocompatibility, respectively. The results obtained were also less than 5% for all the samples (Table 3 and 4) which is within the acceptable range established by Autian, similarly found by XH Qu *et al.* [69-70]. All the samples were found to shown compatibility with the blood. It was interesting to observe a decrement in the % hemolysis with the increase in the concentration of extracellular matrix. There was no significant difference between the samples, yet it was considerably lower than the positive control which showed 100 % hemolysis. The degree of hemolysis, when compared among all the samples, were found to be statistically significant with $p= 0.05$.

1.2.2.7. *In vitro* Cytotoxicity Test:

The biocompatibility/cytotoxicity of the chitosan-ECM composite films was analyzed using the MTT assay that measures the activity of Mitochondrial Succinate Dehyrdogenase enzyme. The general observation is that the activity of the enzyme corresponds to the number of viable cells present. The degree of biocompatibility was expressed as the relative proliferation of the MG63 cells when exposed to films of each blend. This can be viewed in the graphical interpretation as seen in Figure 5. The biocompatibility assay of the polymeric blends showed that the cell proliferation index in all the sets were under acceptable ranges. An increase in the biocompatibility was observed with the increase in ECM concentration in the blended films.

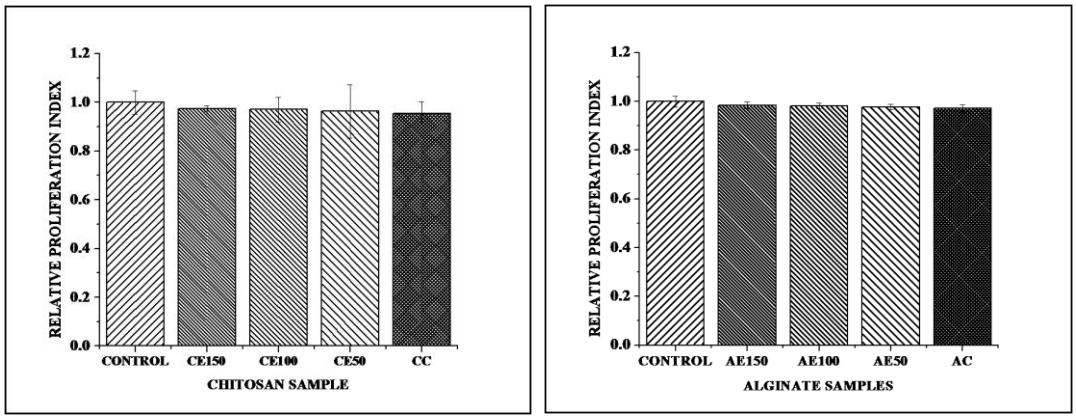

Figure 5. *In vitro* Cytotoxicity test of Chitosan – Extracellular matrix and Alginate – Extracellular matrix composite films

1.2.2.8. Fourier Transform Infrared Spectroscopy:

FTIR analysis was done to see the organic constituent present in the chitosan - ECM films as well as the alginate – ECM films. The graphical interpretation can be seen in Figure 6. Through FTIR, the peaks of amide I, amide II, amide III, CH, CH_2, CH_3, NH, C-O, COO^-, C-N, N-H, and C=O and cross linked C=O functional groups were analyzed. Wave numbers (cm^{-1}) of different functional groups present in Chitosan [71] are given in Table 5, whereas those of functional groups present in collagen, the major component of ECM [72] are tabulated in Table 6.

Table 5: Wave number of different functional groups present in Chitosan

S.NO	FUNCTIONAL GROUPS	WAVENUMBER (cm^{-1})
1	N–H and O–H stretching vibration	3439 cm^{-1}
2	CH_3 symmetric stretch	2925 cm^{-1}
3	C=O stretching vibration	1666 cm^{-1}
4	C–N stretching vibration	1438 cm^{-1}
5	CH_3 bending vibration	1363 cm^{-1}
6	C–O–C bending vibration	1155 cm^{-1}
7	C–OH stretching vibration	1073 cm^{-1}

The Chitosan ECM film samples, when tested through FTIR, showed somewhat similar peaks of chitosan at 3428 cm^{-1} (N-H and O-H stretching bonds), 2949 cm^{-1}(CH_3 symmetric stretch), 1663 cm^{-1} (C=O stretching vibration), 1439 cm^{-1} (C–N stretching vibration), 1365 cm^{-1} (CH_3 bending vibration), 1134 cm^{-1} (C–O–C bending vibration), and 1084 cm^{-1} (C–OH stretching vibration).

Table 6: Wave number of different functional groups present in Alginate

S.NO.	FUNCTIONAL GROUPS	WAVENUMBER(cm^{-1})
1	OH− stretching	3242 cm^{-1}
2	COO^- asymmetric stretching	1596 cm^{-1}
3	COO^- symmetric stretching	1407 cm^{-1}
4	C-O-C anti-symmetric stretching	1081-1024 cm^{-1}
5	carboxyl and carboxylate	1000 to 1400 cm^{-1}

Table 7: Wave number of different functional groups present in ECM

S.NO.	FUNCTIONAL GROUPS	WAVENUMBER(cm^{-1})
1	Amide I region; mainly C=O, C-N bonds	1700-1600
2	Amide II region; mainly combination of C-N stretching and N-H bending vibrations	1600- 1585
3	CH_2 bending vibrations, CH_3 asymmetric bending vibrations, COO^- stretching vibrations, and CH_2 side chains of collagen	1500 – 1300
4	CH_2 side chains vibration	1340
5	Amide III region; mainly C-N stretching, N-H bending, C-C stretching, and sulfate stretching vibrations	1300 – 1180
6	Carbohydrate region: stretching vibrations of C-O, C-O-C, C-OH as well as C-C ring vibrations	1100-1005

Moreover, the presence of ECM was confirmed at 1622 cm^{-1}, 1630 cm^{-1}, 1638 cm^{-1}, and 1644 cm^{-1} (Amide I bands); 1552 cm^{-1}, 1560 cm^{-1}, and 1579 cm^{-1} (Amide II bands); 1259 cm^{-1} (Amide III bands); 1329 cm^{-1}, 1382 cm^{-1}, 1414 cm^{-1}, and 1417 cm^{-1} (CH_2 bending vibrations, CH_3 asymmetric bending vibrations, COO^- stretching vibrations, and CH_2 side chains of collagen); 990 cm^{-1} and 1121 cm^{-1} (Carbohydrate region: Stretching vibrations of C-O and C-OH as well as C-C ring vibrations).

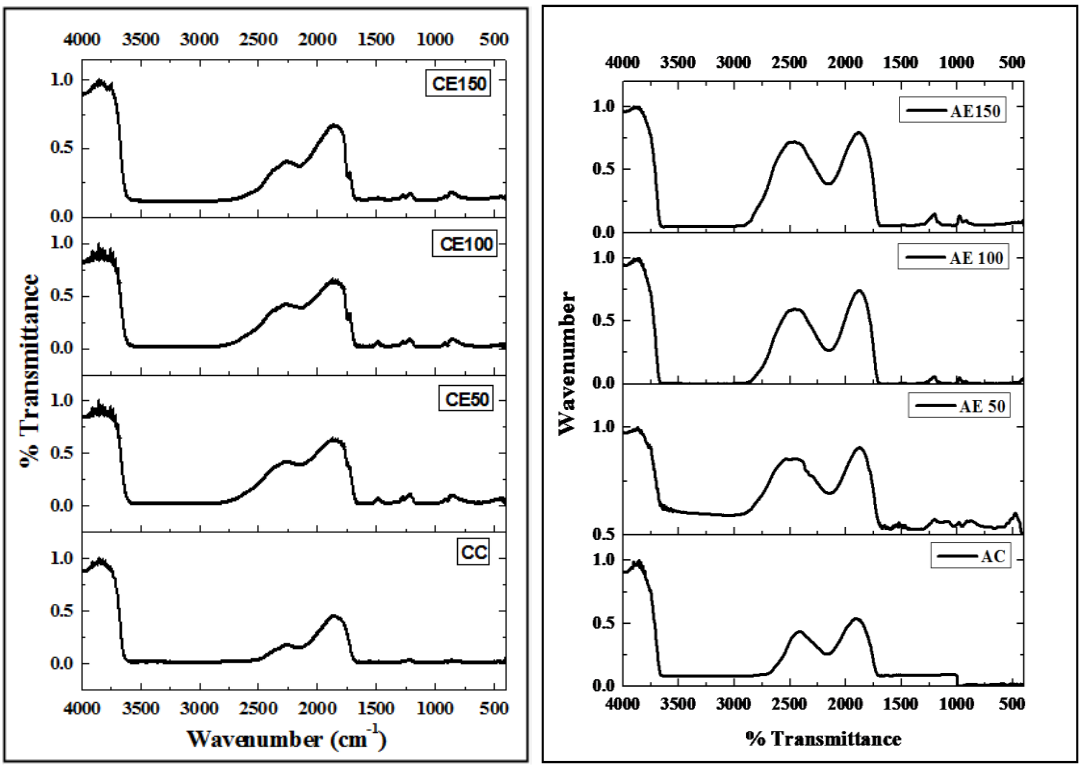

(A) **(B)**

Figure 6. FTIR peak analysis of Chitosan – Extracellular matrix and Alginate – Extracelluar matrix composite films

1.2.2.9 X - Ray Diffraction:

Figure 7 shows the X- ray diffraction pattern of polymer – ECM films. X'Pert Highscore (Version 1.0b, Philips analytical B.V) was used to analyze the diffractograms of the film

samples. According to the literature, the peaks of pure chitosan are generally found near 10° and 20° 2θ [73]. For pure collagen which is a major constituent of ECM, there is a broad diffraction pattern at 10° 2θ and a characteristic peak at 23° 2θ [74]. The typical peaks of chitosan in the chitosan – ECM films were found to be at 11.7° and 26.8° 2θ. Similarly, XRD analysis showed that sodium alginate exhibited a very small crystallinity with peaks at 12°, 23.1°, 31.3°, and 43.8°. Moreover, the presence of ECM in the films was confirmed by the characteristic peaks observed at 22.8°, 26° and 29.16° 2θ with 50mg/ml, 100mg/ml and 150mg/ml ECM concentration respectively. On comparing the diffractograms, it can be observed that as the ECM is introduced in chitosan, there is a strong peak formation, which gets broaden as the ECM increases. This relates to the increase in the amorphous nature of the film. Shift and the broadness of the peak denote that there is certain decrease in the crystallinity.

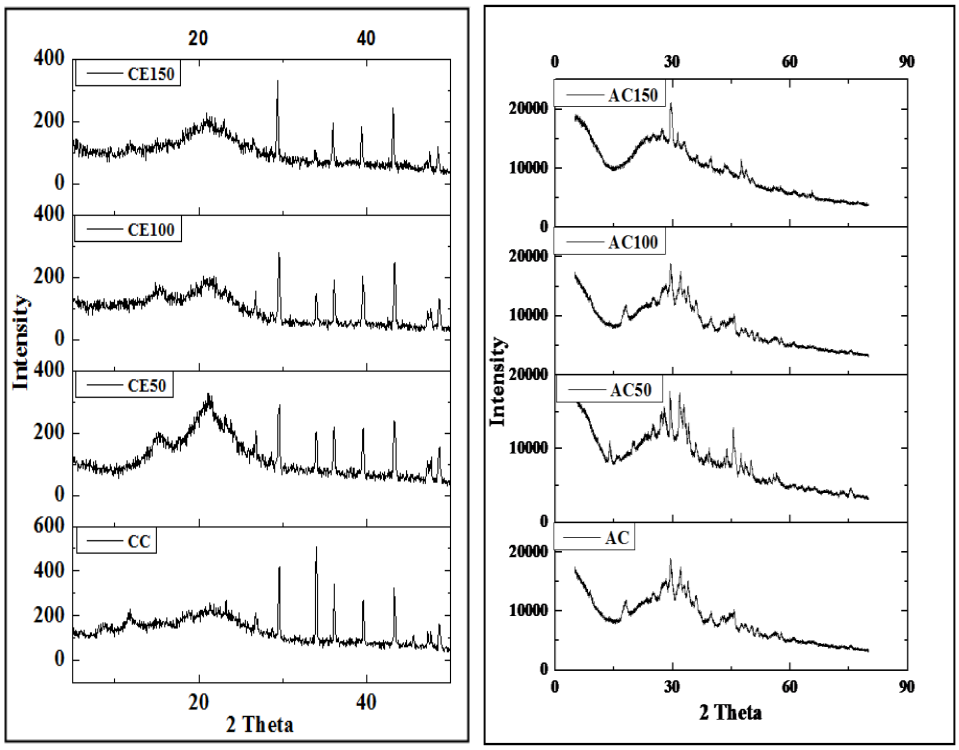

(A) **(B)**

Figure 7. Analysis of XRD pattern in (A) Chitosan – Extracellular matrix and (B) Alginate – Extracellular matrix composite films

4. CONCLUSION

The current study was done to prepare the composite films of Chitosan/ Alginate – porcine omental derived ECM hypothesizing the additive advantages of both for the application in chronic wound healing. The addition of ECM in the chitosan as well as alginate increases the hydrophilicity, hemocompatibility and biocompatibility which have an added advantage over management of chronic wounds. In future, the comparison of the characteristics between the lyophilized and the dried composite films will be made and furthermore immunogenicity of the films will be tested *in vivo.*

II. INSUFFICIENT ANGIOGENESIS

Angiogenesis is a complex and intricate process wherein the pre-existing blood vessels and capillaries give rise to the new ones [75-76]. These blood vessels distribute the nutrients; carry out gas exchange and transport waste, thus maintaining a balanced healthy environment throughout the tissue [77]. Optimally regulated angiogenesis is very essential for proper growth and development of tissue. On the other hand, a deregulated angiogenesis leads to various diseases such as cancer, obesity, diabetes, arthritis, uterine bleedings, Alzheimer's, osteoporosis, stroke, atherosclerosis etc. There exist various chemical mediators like Vascular Endothelial Growth Factors (VEGF), Fibroblast Growth Factor (FGF), Epidermal Growth Factor (EGF), angiostatin, interferon etc. which regulate the angiogenic process [78]. Amongst all such mediators, VEGF is the most prominent inducer of angiogenesis. VEGF is essential for the migration, proliferation and formation of capillary like structures by endothelial cells. VEGF executes its actions by binding to its receptors (VEGFR1 and VEGFR2) on the endothelial cells, thus activating the cascade of many downstream signaling pathways essential for angiogenesis[79]. Chemicals that interrupt this signaling cascade act as angiogenesis inhibitors. Angiogenic inhibitors have potential therapeutic utility in cancer, age related macular degeneration and other diseases where vascular proliferation leads to pathogenesis. Recently, a number of plant derived natural compounds or phytochemicals have been reported to possess a potential anti-angiogenic activity[80-81]. Schindler *et al* and Bagli *et al* reported that the flavonoids like genistein and luteolin have a profound inhibitory effect on VEGF secretion in the cancer cells, thus inhibiting the tumor growth[82-83]. Also, curcumin has been reported for its anti-angiogenic potentials through down-regulation of VEGF expression and inhibition of VEGFRs[84].

Some medicinal plants such as, *Pueraria tuberosa* (Vidarikanda), *Asparagus racemosus* (Shatavari), and *Ficus bengalensis* (Bargad) are historically known to show wide variety of roles in medicinal field. In the current study, we have tried to follow an in silico approach to evaluate the effect of various phytochemicals over the Vascular Endothelial Growth Factor Receptors

(VEGFRs). These tyrosine kinase receptors have an extracellular as well as the intracellular domain. The critical protein models of VEGFR1 and VEGFR2 encoding for both the extracellular domain and intracellular domain have been isolated computationally and were docked with the non – toxic phytochemicals obtained from the above mentioned medicinal plants.

Pueraria tuberosa or Indian Kudzu is widely known in traditional medicines to have many medicinal benefits. It has exhibited cardiotonic, aphrodisiac, anti-hyperglycemic, anti-lipidemic and galactogogue activities [85-88]. Tubers of *Pueraria tuberosa* are rich in Daidzin, Puerarin, Puerarone, genistein, Puetuberosanol, Tuberostan, Tuberosin, and Puerarin 4',6"-diacetate [89-91].Though it has many health beneficial effect but its effect on angiogenesis not been studied much.

Asparagus racemosus, a member of Asparagaceae family is also known as Shatavari. This is one of the endangered species which has been reported to retain the ability to treat number of diseases and disorders. The extracts from various parts of this aryuvedic plant is well known to possess anti-ulcer, anti-bacterial, anti-depressant, anti-inflammatory antiprotozoal, antiviral, antioxidant and antitumorigenic properties [92].

Another plant, *Ficus benghalensis* is an evergreen tree which is distributed all over India. This plant has not only antioxidant properties, but also antitumorigenic, antihelmintic, anti-inflammatory, anti allergic, anti diabetic, analgesic. This plant has also been evaluated for its wound curing abilities as well [93-94].

In the current investigation, we have tried to evaluate the effect of various phytochemicals derived from aforesaid plant source on the Vascular Endothelial Growth Factor Receptors (VEGFRs) using *in silico* approach. The phytochemicals were screened for their toxic and mutagenic effects. Further, the nontoxic and non-mutagenic phytochemicals were docked onto kinase domain of VEGFR1 and VEGFR2.

2.1. MATERIALS AND METHODS

2.1.1. Protein structure retrieval& Active site predictions:

The three dimensional structural models of intracellular kinase domain of VEGFR1 & VEGFR2 proteins were deduced from RCSB Protein Data Bank (http://www.rcsb.org). The cleaning and optimization of the protein model geometry was carried out by removal of miscellaneous ligands

and other hetero-atoms such as water, ions etc. using Argus Lab Software. Further, the protein models were used for the active site prediction using CASTp Calculations (Computed Atlas of Surface Topography of proteins) (http://stsfw.bioengr.uic.edu/castp/calculation.php). Amongst all predicted sites, the site having the catalytic amino acids was selected for docking. The clue about the amino acids involved in protein catalysis was gained from UniProt Server (http://www.uniprot.org/).

2.1.2. Substrate selection:

The three dimensional PDB structures of the phytochemicals present in the aforesaid plants and the standard FDA approved drug molecules were retrieved from KNApSAcK-3D (http://knapsack3d.sakura.ne.jp/) and PubChem (http://pubchem.ncbi.nlm.nih.gov/) databases using PRODRG Server (http://davapc1.bioch.dundee.ac.uk/prodrg/). Further, energy minimization & ligand optimization was carried out using Argus lab software.

2.1.3. Molecular Property Predictions:

The selected phytochemicals were examined for their molecular properties, ADME and toxicity using PreADMET (http://preadmet.bmdrc.org/).The phytochemicals which passed the selection criterion were used for the docking analysis.

2.1.4. Molecular Docking:

The selected phytochemicals were docked into the active sites of the protein models using AutoDock4.2 software tool. In brief, polar hydrogen and Kollman charges were added to the protein models and docking was done by Lamarckian Genetic Algorithm using standard protocol based on the population size of 150 haphazardly located individuals; a maximum number of $2.5*10^7$ energy evaluations, with 0.02 mutation rate and 0.8 crossover rate [95]. Twenty independent docking runs were carried out and results were clustered according to the 1.0 Å RMSD criteria. Auto gridding was done in the grid maps of proteins, setting the grid size of 60*60*60 points along with grid spacing of 0.375 Å. This was followed by the visualization of the interaction details in the protein-ligand complex using UCSF chimera [96] and LigPlot$^+$ [97].

2.1.5. Extraction of the Phytochemicals:

Asparagus racemosus and Ficus benghalensis were selected for the extraction of the phytochemicals due to the availability of these plants. The plants were washed thoroughly two to three times. The required portion of the plant was taken and cut into tiny pieces which were made into powder using liquid N_2. The powder was loaded in the thimble paper and placed in the porous container of the soxhlet apparatus. Complete set up was prepared and started. The extract gets filtered and gets collected in the distilled pot which is collected. The extract is dried using a vacuum evaporator and was stored in dark at 4°C. The extract having the phytochemicals were tested for their presence through the biochemical analysis. The Phytochemical screening was carried out by the method of Harborne, 1973. A stock solution of concentration 1 mg/ml was used as the extract for the phytochemical analysis [98-99].

- **Test for carbohydrates:**

To 2 ml of extract, 1 ml of Molisch's reagent and few drops of concentrated hydrochloric acid were added. The appearance of reddish colour indicates the presence of carbohydrates.

- **Test for tannins:**

For testing the presence of tannins, 2 ml of 5 % ferric chloride was added to 1 ml of the plant extract. The appearance of dark blue or greenish blue colour showed the presence of tannins.

- **Test for saponins:**

The presence of saponins was confirmed by adding 2 ml of distilled water to 2 ml of plant extract, followed by shaking in a graduated cylinder for about 15 minutes. There is a formation of about 1 cm layer of foam indicates the presence of saponins.

- **Test for flavonoids:**

The appearance of yellow colour indicated the presence of flavonoids when 1 ml of 2N sodium hydroxide was added to 2 ml of the plant extract.

- **Test for alkaloids:**

To 2 ml of extract, 2 ml of Wagner's reagent were added. The appearance of reddish brown colour precipitate confirms the presence of alkaloids.

- **Test for quinines:**

To 1 ml of extract, 1ml of concentrated sulphuric acid was added. The appearance of red color indicates the presence of quinones.

- **Test for steroids:**

Test for steroids included the addition of 1 ml of chloroform and few drops of concentrated hydrochloric acid to 1 ml of extract. The formation of brown ring at the interface confirms the presence of steroids.

- **Test for terpenoids:**

To 0.5 ml of extract, 2 ml of chloroform and few drops of concentrated hydrochloric acid were added. The formation of red brown color at the interface indicates the presence of terpenoids.

2.1.6. Cell Proliferation Assay:

The phytochemicals which were came out to be the better ones, were chosen for the in vitro analysis. Cell proliferation assay was done to check the effects of these phytochemicals. These were taken in two sets- one of higher concentrations and the other, the lower ones. 96 well plates were seeded which were loaded with the concentrations of the drug or phytochemical after 24 hrs. MTT assay was done from 0^{th} day to 4^{th} day. The absorbance of all the samples was taken and relative proliferation index was calculated.

2.2. RESULTS & DISCUSSIONS

2.2.1. *In silico* analysis:

VEGFR1 and VEGFR2 are the transmembrane tyrosine kinase receptors with all the three domains: extracellular domain, transmembrane region, and an intracellular domain. Although VEGFR1 was earlier considered as a negative regulator of VEGFR2, but recently it was also found to cause the accumulation of the angioblast cells in the blood vessels. On the other hand, VEGFR2 plays a primary role in angiogenesis, vascular permeability and differentiation of the above mentioned angioblast cells [100].

Usually, the FDA approved anti-angiogenic drugs are targeted at the intracellular domain of the VEGFRs, including the ATP binding domain. ATP binding domain gains a special attention while considering receptor tyrosine kinases as ATP hydrolysis plays a crucial role in their activation. Thus, inhibition of this domain may potentially inhibit the signaling pathways. Keeping this prospective in mind, we evaluated the inhibitory potentials of phytochemicals by blocking the ATP binding domain of VEGFRs. Recently, interaction between juxtamembrane domain and catalytic domain of VEGFR2 has gained a significant attention. Juxtamembrane domain connects the transmembrane domain with the catalytic intracellular domain in receptor tyrosine kinases [101]. James Solowiej *et al* have reported that the presence of the Juxtamembrane domain of VEGFR2 has a substantial effect on inhibitor binding to the catalytic domain of VEGFR2. It was observed that presence of juxtamembrane domain enhanced the affinity of Axitinib for the catalytic domain of VEGFR2 [102]. However, absence of an intact X-Ray crystallographic structure for the same, limits it use for the present *in silico* investigation. Thus, three dimensional structures of catalytic domain of VEGFR1 (3HNG) and VEGFR2 (3VHE) were taken for the analysis from RSCB PDB (Table 8). For *in silico* analysis of the ligand-protein interaction, the knowledge of active site of the protein is essential because ligands usually target the active sites. The active site of proteins was predicted using CASTp Calculations.

Table 8: Targets to check the effect on Angiogenesis

Proteins	Notations	PDB ID	Organism	Ref.
Vascular Endothelial Growth Factor Receptor 1	VEGFR1	3HNG	*Homo Sapiens*	[103]
Vascular Endothelial Growth Factor Receptor 2	VEGFR2	3VHE	*Homo Sapiens*	[104]

The three dimensional structure of phytochemicals was isolated from KNApSacK-3D & PubChem database. Screening of the phytochemicals was carried out using PreADMET server and was based on their molecular properties including drug likeness, carcinogenicity and

mutagenicity. The ligands which passed the selection criteria were further subjected to docking analysis. Eighteen out of one hundred forty molecules were found to be non-toxic and were used for docking study using AutoDock4.2. Non-toxic eighteen molecules were docked with the intracellular domain of VEGFRs, within which Puerarone and Tuberostan gave best binding with VEGFR1 and VEGFR2. Further study was continued with these two molecules. The origin and chemical structures of these molecules is mentioned in Table 9.

Table 9: Name and the origin of the selected phytochemicals

KNApSAcK ID	Name of the Phytochemical	Origin	Ref
C00009871	Puerarone	*Pueraria tuberosa* (Vidarikanda)	[105]
C00010049	Tuberostan	*Pueraria tuberosa* (Vidarikanda)	[106]
C00034434	Asparagamine A	*Asparagus racemosus* (Shatavari)	[107]
44257152	Leucopelargonidin 3 - O - glucoside	*Ficus bengalensis* (Bargad)	[108]

Puerarone and Tuberostan, both were found to follow Lipinski's rule of five which permit the assessment of pharmacokinetics of the drug including absorption, distribution, metabolism and excretion (ADME). Furthermore, they were recognized as non-toxic, non-mutagenic and non-carcinogenic in nature (Table 10).

Table 10: Molecular properties of the selected phytochemicals

PROPERTIES	Puerarone	Asparagamine A	Tuberostan	LPGG
Molecular weight (gm/mol)	336.33804	385.45	348.34874	452.40866
Log P	5.09	2.24	5.87	-1.97
HB donor	2	1	0	8

HB acceptors	5	6	5	11
AMES Test	Non Mutagen	Non Mutagen	Non Mutagen	Non Mutagen
Carcinogenicity	Non Carcinogen	Non Carcinogen	Non Carcinogen	Non Carcinogen
Human Intestinal Absorption (%)	93.881	90.947	95.894	14.96
In Vitro Plasma Protein Binding (%)	94.938	44.936	89.858	67.229

Puerarone (KNApSAcK_3D ID C00009871) displayed best affinity towards the intracellular domain of VEGFR1 with binding energy of -9.91 kcal/mol (Ki: 0.182 µM). On the other hand, Tuberostan (KNApSAcK_3D ID C00010049) showed highest affinity towards the intracellular domain of VEGFR2 with binding energy of -9.32 kcal/mol (Ki: 0.148 µM). When compared with all the FDA approved drugs as mentioned in the table , it was found that Puerarone showed better binding affinity with VEGFR1 intracellular domain with the exception of Pazopanib and Vatalanib where it showed comparable results. Similarly, Tuberostan showed better results than all the drugs except Pazopanib and Axitinib where it showed almost equal results. In table 11, red colored values represents best affinity of the test molecules with the intracellular domain of VEGFR1 and VEGFR2.

As per Asparagamine A (KNApSAcK_3D ID C00034434) is concerned, it showed binding of -8.74kcal/mol (Ki: 0.194). Similarly, Leucopelargonidin 3-o-glucoside (LPGG) showed binding affinity of -7.36kcal/mol (Ki: 2). In VEGFR2, Asparagamine A and LPGG showed binding of -8.24 (Ki: 0.456) and -7.7 kcal/mol (Ki: 1.13).

Table 11: Binding interaction of VEGFR1 and VEGFR2 with selected phytochemicals.

PDB ID	**Ligands**		**Minimum Binding Energy (kcal/mol)**	**Ki (µM)**	**Hydrogen Bonds**	**Interacting Amino Acids**
VEGFR1						
3HNG	Test molecule	Puerarone	-9.91	0.182	0	-
		Tuberostan	-8.44	0.646	0	-
		Asparagamine	**-8.74**	**0.194**	0	-

	Standard Inhibitors	A Leucopelargonidin 3-o-glucoside	**-7.36**	**2**	6	Asp807, Glu878, Cys1018, Asp1040, Leu1043
		Sunitinib	-7.44	7.0	3	Cys912 (2), Cys1039
		Pazopanib	-10.19	0.034	3	Lys861, His1020, Asp1040
		Axitinib	-9.86	0.059	3	Cys1018, Asp1040 (2)
		Vandetanib	-8.54	0.5493	0	-
		Vatalanib	-12.18	0.0018	3	Glu878, Cys912, Asp1040
		Sorafenib	-9.44	0.120	3	Cys912(2), Asp1040
VEGFR2						
3VHE	Test molecule	Puerarone	-7.91	1.58	1	Cys1045
		Tuberostan	-9.32	0.148	0	-
		Asparagamine A	**-8.24**	**0.456**	1	Asp1046
		Leucopelargonidin 3-o-glucoside	**-7.7**	**1.13**	5	Asp814, Cys817, Ala881
	Standard Inhibitors	Sunitinib	-6.26	51.98	4	Asp814, Lys868, Ala 881, Leu1049
		Pazopanib	-9.58	0.095	1	Asp1046
		Axitinib	-9.94	0.052	1	Lys868
		Vandetanib	-7.36	4.01	0	-
		Vatalanib	-8.78	0.367	1	Asp1046
		Sorafenib	-7.7	2.26	1	Lys868

For an effective binding of a ligand with a protein receptor, the affinity of the ligand towards the protein as well as the stability of the protein ligand complex, are some of the important benchmarks. The above mentioned binding energies along with the interaction profile (hydrogen bonds & hydrophobic interactions) provide an important indication for the affinity and stability of ligand with the protein. The hydrogen bonds and hydrophobic interactions formed between proteins and phytochemicals were illustrated through LigPlot^{+} (Table 12). Interaction profiles were figured out only for the best possible orientation of the selected ligand molecule. For LigPlot+ analysis, an illustrative figure was generated for each ligand, describing bonded as well as non – bonded interactions between the ligands and protein.

Table 12: Binding interaction of VEGFR1 and VEGFR2 extracellular domain with selected phytochemicals.

PDB ID	Ligands		Hydrogen Bonds	Hydrophobic Interactions
VEGFR1				
3HNG	Test molecules	Puerarone	Glu878, Glu910	Leu833, Val841, Ala859, **Lys861**,Leu882, Val892, Val907, Val909, Tyr911, Cys912, Gly915, Leu1029, Cys1039, Phe1041
		Tuberostan	-	Leu833, Val841, Ala859, **Lys861**, Glu878, Ile881, Leu882, Ile885, Val892, Val907, Val909, Cys1018, Leu1029, Ile1038, Cys1039, Asp1040
		Asparagamine A	Asp1040	Ala874, Thr877, Glu878, Ile881, Leu882, Val892, Cys1018, His1020, Ile1038, Cys1039, Gly1042
		LPGG	Asp807, Glu878, Asp1040	Thr877, Ile881, Ile885, Leu1013, Cys1018, Gly1042, Leu1043
	Standard Inhibitors	Sunitinib	Cys912 (2), Cys1039	Leu833, Val841, Ala859, Glu878, Leu882, Val907, Val909, Glu910, Tyr911, Gly915, Asn916, Leu1029, Asp1040, Phe1041
		Pazopanib	Asp1040	Leu833, Val841, **Lys861**, Glu878, Val892, Val909, Tyr911, Cys912, His1020, Leu1029, Cys1039, Phe1041
		Axitinib	Asp1040 (3)	Asp807, Lys861, Glu878, Ile881, Leu882, Vaal892, Cys1018, Ile1019, His1020, Arg1021, Ile1038, Cys1039
		Vandetanib	-	Val841, Glu878, Ile881, Leu882, Ile885, Val891, Val892, Val909, Leu1013, Leu1029, Ile1038, Cys1039, Asp1040, Phe1041
		Vatalanib	Glu878, Cys912, Asp1040 (2)	Leu833, Ala859, **Lys861**, Leu882, Val891, Val907, Val909, Glu910, Tyr911, Leu1013, Leu1029, Ile1038, Cys1039, Phe1041
		Sorafenib	Cys912, Asp1040	Leu833, Val841, Ala859, **Lys861**, Glu878, Ile881, Leu882, Val892, Val909, Glu910, Tyr911, Gly915, Leu1013, Cy1018, Cys1039

VEGFR2				
3VHE	Test molecules	Puerarone	Glu885, Cys1045	Leu840, Val848, Ala866, **Lys868**, Lue889, Val916, Gly922, Asn923, Lue1035, Asp1046, Phe1047
		Tuberostan	-	Lue840, Val848, **Lys868**, Glu885, Leu889, Val899, Val916, Phe918, Cys919, Lys920, Gly922, Cys1045, Asp1046, Phe1047
		Asparagamine A	Asp1040	Ala874, Thr877, Glu878, Ile881, Leu882, Val892, Cys1018, His1020, Ile1038, Cys1039, Gly1042
		Leucopelargonidin 3-o-glucoside	Asp807, Glu878, Asp1040	Thr877, Ile881, Ile885, Leu1013, Cys1018, Gly1042, Leu1043
	Standard Inhibitors	Sunitinib	Asp814, Lys868, Ala 881, Leu1049	Cys817, Leu882, Ser884, Glu885, Ile888, Asp1046, Gly1048
		Pazopanib	Asp1046	Val848, Ala866, Val867, **Lys868**, Glu885, Ile888, Leu889, Val899, Val914, Val916, Cys919, Gly922, Leu1035, Cys1045, Phe1047
		Axitinib	Asp1046	Leu840, Val848, Ala866, **Lys868**, Glu885, Leu889, Val899, Val916, Phe918, Cys919, Gly922, Leu1035, Cys1045, Phe1047
		Vandetanib		**Lys868**, Glu885, Ile888, Leu889, Val899, Val916, Leu1035, Cys1045, Asp1046, Phe1047, Gly1048
		Vatalanib		Val848, **Lys868**, Glu885, Leu889, Val899, Val914, Val916, Leu1035, Cys1045, Asp1046, Phe1047
		Sorafenib	Lys868	Leu840, Val848, Ala866, Glu885, Leu889, Val899, Val916, Glu917, Cys919, Phe918, Leu1035, Cys1045, Asp1046, Phe1047(2), Gly1048

The hydrophobic amino acids of the intracellular domain of VEGFR1, which are engaged in the hydrophobic interactions with Puerarone, are Leu833, Val841, Ala859, Lys861, Leu882, Val892, Val907, Val909, Tyr911, Cys912, Gly915, Leu1029, Cys1039, and Phe1041. Within the commercial inhibitors, Vatalanib bound with the VEGFR1 intracellular domain more strongly than the others. Interestingly, the interaction profile of Vatalanib interacted hydrophobically with

Leu833, Ala859, Lys861, Leu882, Val907, Val909, Tyr911, Leu1029, Cys1039, and Phe1041, and formed hydrogen bonds with Glu878 which was similar to that of Puerarone. It is important to mention that Asp1040 residue of VEGFR1 was involved in hydrogen bond formation with Pazopanib, Axitinib, Vatalanib and Sorafenib. Lys861 forms a major amino acid residue of ATP binding sites in intracellular domain VEGFR1 and interestingly both, Puerarone and most of the inhibitors interacted with it. This provides us the clue that Puerarone may block the ATP binding site of VEGFR1, thus enforcing their inhibitory effect.

Equivalently, Tuberostan was found to interact more effectively with the intracellular kinase domain of VEGFR2 through eleven hydrophobic amino acids, including Leu833, Lue840, Val848, Lys868, Glu885, Leu889, Val899, Val916, Phe918, Cys919, Lys920, Gly922, Cys1045, Asp1046, and Phe1047. Among the inhibitors, Axitinib showed the highest affinity for intracellular domain of VEGFR2. Both Tuberostan and Axitinib were found to share their hydrophobic interactions with Leu840, Val848, Lys868, Glu885, Leu889, Val899, Val916, Phe918, Cys919, Gly922, Cys1045, and Phe1047. Also, Tuberostan formed hydrophobic interaction with Asp1046, which on the contrary, was involved in the hydrogen bonding with Axitinib. Similar to VEGFR1, Lys868 forms a crucial residue for ATP binding in the case of VEGFR2 which was recognized to show hydrophobic bonding with Tuberostan and commercial inhibitors. Both the proteins as well as all the inhibitors showed hydrophobic interaction at the ATP binding site but Tuberostan, in addition, showed maximum hydrophobic interaction and highest binding affinity as per the LigPlot^{+} and Chimera analysis. Thus, making it better candidate for inhibition of intracellular domain of VEGFR2. The interaction profile of the phytochemicals with the VEGFRs using Autodock4.0, Chimera and LigPlot+, can be viewed in Fig 8.

Asparagamine A, though showed less binding affinity with the VEGF receptors, but showed a very good hydrophobic interactions with Leu833, Val841, Ala859, Lys861 (active site) , Glu878, Ile881, Leu882, Ile885, Val892, Val907, Val909, Cys1018, Leu1029, Ile1038, Cys1039, Asp1040. Similarly with VEGFR2, Asparagamine A showed interactions with Val848, Ala866, Lys868 (active site), Glu885, Ile888, Leu889, Ile892, Val899, Val916, Leu1035, Ile1044, Cys1045, and Phe1047.

LPGG showed hydrophobic interactions with VEGFR1, involving Thr877, Ile881, Ile885, Leu1013, Cys1018, Gly1042, and Leu1043. With VEGFR2, LPGG interacted with Leu840,

Val848, Ala866, Lys868 (active site), Leu889, Val899, Val916, Cys919, Lue1035, Cys1045, Asp1046, and Phe1047. It can be observed that Asparagamine A and LPGG, both were having interactions with the active site, which can have a very crucial effect over the receptors, thus affecting angiogenesis. Due to the unavailability of *Pueraria tuberosa*, the work was continued with *Asparagus racemosus* and *Ficus benghalensis*.

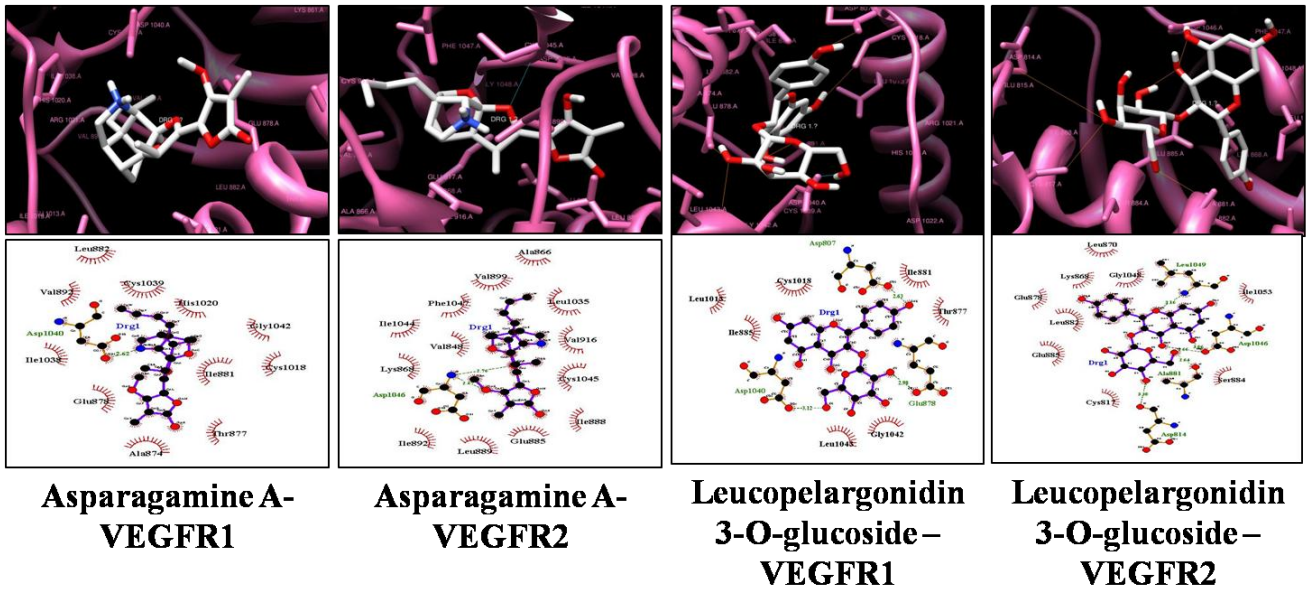

Figure 8. Interaction Profile of phytochemical Asparagamine A and Leucopelargonidin 3-o-glucoside with VEGF receptors using Chimera and LigPlot+

2.2.2. Extraction of Phytochemicals:

The plant was taken and the extraction of the plant was done using soxhlet apparatus. The extract was dried in vacuum evaporator and stored. For this purpose, the extraction was done using the soxhlet, commonly known as the solvent extraction. This solvent extraction is a procedure that can be used to detach or isolate the sample from the plant containing many other impurities. Choice of solvent is based on the phytochemicals required from the plant. *Asparagus racemosus* and *Ficus benghalensis* were extracted using methanol as well as aqueous solvents [109].

Figure 9: Extraction of phytochemicals from *Asparagus racemosus* using soxhlet method

The plant extracts do not have only one phytochemical but have a mixture of many. For having expected phytochemicals were examined for their presence using the biochemical tests which is tabulated in Table 13.

Table 13: Phytochemical analysis of the plant extracts of *Asparagus racemosus* and *Ficus benghalensis*

S.NO	NAME OF THE TEST	EXPECTED COLOUR	RESULT	
			Asparagus racemosus	*Ficus benghalensis*
1	Test for carbohydrates	Reddish Colour	++	++
2	Test for tannins	Dark Blue Colour	-	-
3	Test for alkaloids	Yellow colour ppt	+++	++
4	Test for Flavonoids	Yellow Colour	+++	+++
5	Test for terpenoids	Reddish Brown at interface	+	-
6	Test for saponins	Foam appears	-	+
7	Test for quinines	Red Colour	-	+
8	Test for steroids	Brown ring at interface	+	+

***+++ Highly present ; ++ Moderately present ; - not present**

2.2.3. Cell proliferation assay:

After the complete biochemical analysis, the phytochemicals are needed to be tested for the amount it should be used. There two different sets of different concentrations were taken. MTT assay was done to check the cell proliferation in the presence of the extract. These were compared for their relative proliferative index in which it was found that the concentration at micrograms are more compatible for the cells and even help in the cell proliferation. The cells were found to die at higher concentrations of the phytochemicals. The concentrations found through the in silico analysis was confirmed here as the Ki values of these plants are also equal and less than the µM concentrations.

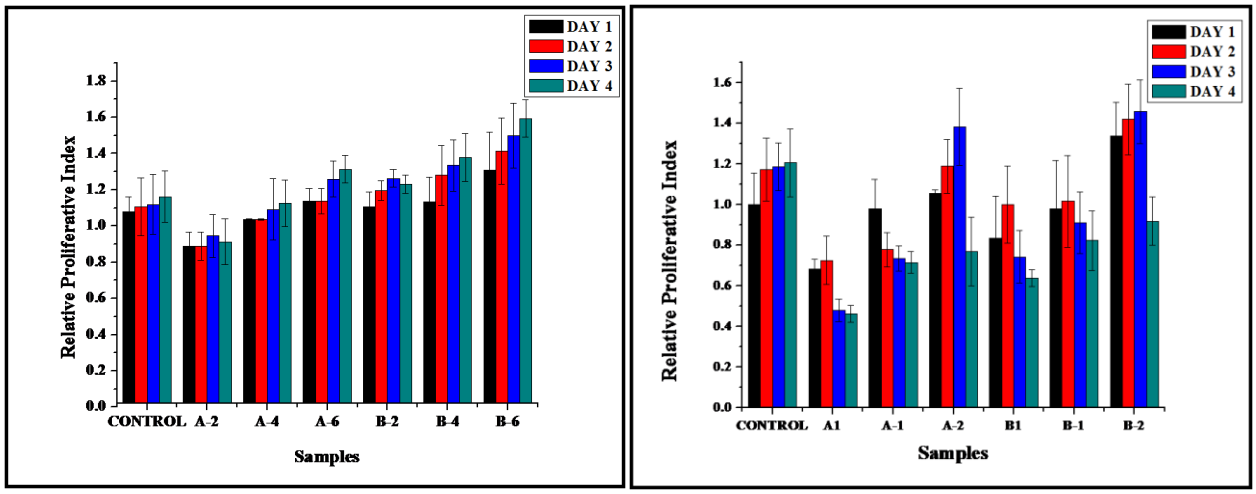

Figure 10: Optimization of the concentration of the phytochemicals for their effect over the cell proliferation. *Asparagus racemosus*: A1=1mg/ml; A-1= 10^{-1}mg/ml; A-2=10^{-2}mg/ml; A-4=10^{-4}mg/ml; A-6= 10^{-6}mg/ml. *Ficus benghalensis*: B1=1mg/ml; B-1= 10^{-1}mg/ml; B-2=10^{-2}mg/ml; B-4=10^{-4}mg/ml; B-6= 10^{-6}mg/ml.

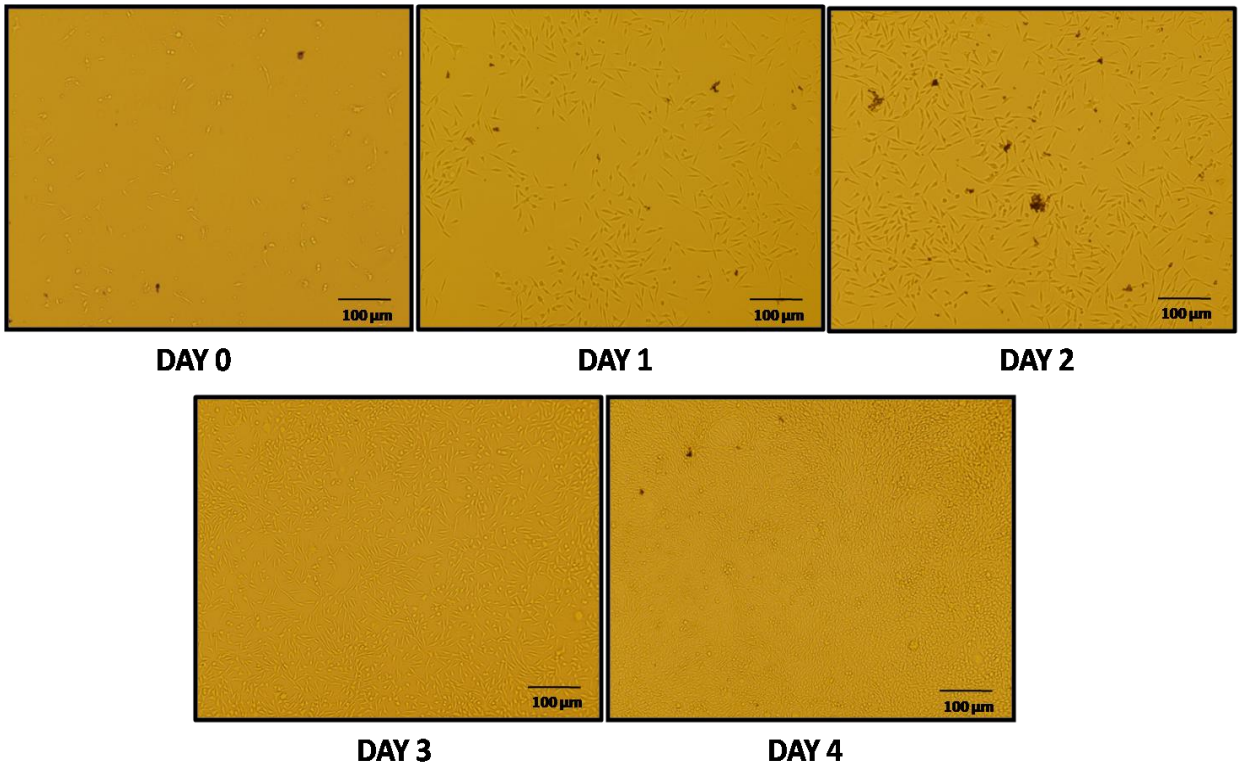

Figure 11: Cell proliferation in the presence of the microgram concentration of the plant extract.

It was observed that at high concentration of the extract, the cell started dying after 4^{th} day of cell proliferation. On the other hand, the low concentration of the extract initiated the proliferation of the cells very well. The dilutions of the concentration till the microgram concentration were done as the required phytochemical Asparagamine A and LPGG obtained from the *in silico* study, had Ki in micromolar concentrations. *In silico* study was confirmed and was identical with the one prepared *in vitro*. Though it was a crude extract but the concentration was maintained at around microgram which was not toxic to the cells, rather it enhanced the rate of proliferation. The proliferation of cells which usually takes 6-7 days to become completely confluent but it was completed in 4days. The samples having lowest concentration of the extract was found to support the cell proliferation. It can also be estimated that more the proliferation of cells, more is the secretion of growth factors like VEGFs and FGFs, more is the angiogenic potential. But still the optimization of angiogenic potential is need through the VEGF expression assay.

CONCLUSION:

In this complete study *in silico* was done to elucidate the medicinal potentials of the phytochemicals derived from herbal plants. The overall analysis suggested that Asparagamine A and Leucopelargonidin 3-o-glucoside could show good affinity towards the critical proteins VEGFR1 and VEGFR2 respectively. The study provided a new direction for the designing and development of a novel drug against VEGFRs for the treatment of multiple angiogenic diseases; thus using the pharmacological aspects of these compounds. Further, *In vitro* and *In vivo* study over the cell proliferation proved it to be non toxic at the level of microgram/ ml concentration, thus initiating a good proliferation rate than the usual rate, without the involvement of the phytochemicals. *In vitro* as well as *in vivo* validation of the estimated mechanism as well as the therapeutic potentials of the selected phytochemicals is required through the VEGF expression assay.

III. INSUFFICIENT ADIPOGENESIS

Adipose tissue is not only known for its abundance in the human body but also as a major reserve for energy, and storage of triacylglycerol. Adipose tissue includes cells known as adipocytes along with the fibroblast cells, smooth muscle cells, endothelial as well as adipogenic progenitor cells. These adipocytes which are specialized cells for adipose tissue, release various growth factors that are important in the regulation of many pathways. The pre-adipocyte differentiation upto mature adipocyte is due to the regulation of two major factors, C/EBPs and PPARγ. In addition, Peroxisome Proliferator activated receptors as well as the CCAAT/ enhancer binding protein; both regulate each other also [110-112].

Among all, PPARγ is important for adipogenesis as it not only affect the differentiation of the preadipocytes but also initiate the storage of fatty acids in the differentiated adipocytes. PPARγ is present in two isoforms- γ1 and γ2. Though γ1 is expressed in majorly all the tissues but still it plays fewer roles in adipogenesis as γ2. Recently it has been found that the over-expression of the latter, can lead to disorders like Cancer, Obesity. On the contrary, the problems like severe burns or in traumatic wound, healing is required and at that time there is need of adipogenesis, especially in deep wounds or deep burns.

In the current study, the in –silico analysis was tried to test the effect of the phytochemicals over the adipogenesis through the molecular docking analysis of these phytochemicals with PPARγ.

3.1. MATERIALS AND METHODS

3.1.1. Protein structure retrieval:

Protein Data Bank was used to retrieve the three dimensional crystal structures of the target protein (http://www.rcsb.org/pdb/). Table 1 lists the proteins studied for the targeted disease. Removal of miscellaneous ligands and other hetero-atoms such as water molecules, ions, atoms, etc. was done from the protein models for a better active site predictions and analysis, followed by further docking studies using Argus Lab Software.

3.1.2. Protein Active Site Predictions:

CASTp Calculations (Computed Atlas of Surface Topography of proteins) were used for predicting the active sites of the target proteins. Amongst the predicted site, the site having the catalytic amino acids was chosen for the docking of the ligand. The catalytic amino acids of the each protein were analyzed from UniProt (http://www.uniprot.org/).

3.1.3. Substrate selection:

The three dimensional structure of Asparagamine A was screened from KNApSAcK-3D database (http://knapsack3d.sakura.ne.jp/). The PDB structure of the ligand was deduced using PRODRG Server (davapc1.bioch.dundee.ac.uk/cgi-bin/prodrg). Optimization of the ligands and the minimization of their energy were done using Argus lab software. Besides, the standard or reference molecules were also evaluated. For which, the three dimensional structures of standard molecules for all the aforesaid proteins were also deduced from PubChem database (http://pubchem.ncbi.nlm.nih.gov/) and were used as reference molecules.

3.1.4. Molecular Properties and Drug likeness:

The Asparagamine A was further examined for its drug likeness and molecular properties using FAF-Drug2 (http://mobyle.rpbs.univ-paris-diderot.fr/cgi-bin/portal.py?form=FAF Drugs#forms:: FAF- Drugs2) and PreADMET (http://preadmet.bmdrc.org/).

3.1.5. Molecular Docking:

The computational docking of Asparagamine A and standard inhibitors were performed into the active site of corresponding protein models using AutoDock4.2 software (version 1.5.6). While docking, polar hydrogen's were added to protein models using the hydrogen's module and thereafter, Kollman united atom partial charges were assigned. Docking of ligand was carried out using Lamarckian Genetic Algorithm with standard docking protocol on the basis a population size of 150 randomly placed individuals; a maximum number of $2.5*10^7$ energy evaluations, a mutation rate of 0.02, a crossover rate of 0.80 and an elitism value of 1 [113]. Fifteen independent docking runs were carried out for each ligand and results were clustered according to the 1.0 Å rmsd criteria. The grid maps representing the proteins were calculated using autogrid and grid size

was set to 60*60*60 points with grid spacing of 0.375 Å. The coordinate of the docked protein along with the ligand was visualized using UCSF chimera and LigPlot^{+} [114].

3.2. RESULTS AND DISCUSSION:

The molecular docking analysis was done which gave the top binding ligands which were further compared with the standard known drug molecules.

From the docking analysis of the phytochemicals with PPAR γ, it was found that previously selected phytochemicals gave very good results with PPAR γ as well. Chimera analysis showed the binding interactions which revealed the hydrogen interactions which the ligands made with the protein (Table 14). Asparagamine A, a unique phytochemical present in *Asparagus racemosus* showed the binding of -9.90Kcal/mol with Ki 0.522 µM. This ligand showed interactions with PPAR γ involving Cys285, Glu286, Ser289, His323, and Tyr473. LPGG showed less but effective binding affinity of -7.60 Kcal/mol (Ki: 2.67) with PPAR γ involving Ser289, and His 323.

Table 14: Binding interaction of PPAR gamma with selected phytochemicals.

PDB ID	Ligands	Minimum Binding Energy (kcal/mol)	Ki (µM)	Interacting Amino Acids
3ET3	Asparagamine A	-9.90	0.522	Cys285, Glu286, Ser289, His323, Tyr473
	Quercitrin	-9.52	0.105	Cys285, Gln286, Ser289, Tyr327
	Leucopelargonidin 3-o glucoside	-8.38	2.06	Ser289, His 323
	Isoquercitrin	-7.60	2.67	Ser 289, Phe360,Tyr473, His449

Similarly, Isoquercitrin commonly found in *Centella asiatica* (Mandukaparni) showed binding of -8.38Kcal/mol (Ki: 2.06) through amino acids Ser 289, Phe360, Tyr473, and His449 . *Centella asiatica* is also known as Brahmi, is majorly used in lesions and infections. It is also used as

wound healer. Quercitrin which is mainly found in *Cressa cretica* as well as Centella asiatica mentioned above, showed binding affinity of -9.52Kcal/mol (Ki: 0.105). This ligand interacted with the protein Cys285, Gln286, Ser289, and Tyr327. *Cressa cretica* is also one of a medicinal plant, known as Rudravanti is famous for its therapeutic properties for treating asthma, diabetes and skin diseases. LigPlot+ analysis revealed the hydrophobic interactions of ligands with PPARγ that can be viewed in table 15.

Table 15: Molecular interactions of PPAR gamma with phytochemicals revealing the hydrogen and hydrophobic interactions using LigPlot+

PDB ID	Ligands	Hydrogen Bond Interaction	Hydrophobic interaction
3ET3	Asparagamine A	Cys 285, Glu286, Ser289, His323, Tyr473	Ile281, Phe282, Arg288, Ile326, Tyr327, Leu330, Leu353, Leu256, Phe363, Met364, Lys367, Leu465, Leu469
	Quercitrin	Cys285, Gln286, Ser289, Tyr327	Ile281, Phe282, Ile326, Arg288, Leu330, Leu356, Phe363, Met364, Lys367, His449, Leu465, Leu469,
	Leucopelargonidin 3-o glucoside	Ser289, His 323	Phe282, Cys285, Ile326, Tyr327, Leu330, Val339, Ile341, Met364, Lys367, His449, Leu453, Leu465, Leu469, Tyr473
	Isoquercitrin	Ser 289, Phe360,Tyr473, His449	Ile281, Arg288, Phe282, Ile326, Leu330, Leu356, Phe363, Met364, Lys367, His449, Leu465, Leu469

The analyzed ligands were also compared with the reference molecules which proved the phytochemicals as an effective ligand for PPARγ. The binding interactions for the reference molecules can be viewed in table 16.

Table 16: Binding interaction of PPAR gamma with standard molecules.

Proteins	Reference molecule	Minimum Binding Energy (Kcal/mol)	Ki (μM)
PPARγ	MK886 [115]	-9.28	0.158
	Thiazolidine-2,4-dione [116]	-4.01	1140

The binding pattern or the interaction profile of all the ligands were noted and can be viewed in figure 11. This analysis involved the use of Chimera and LigPlot+ for the hydrogen bonds and hydrophobic interaction study.

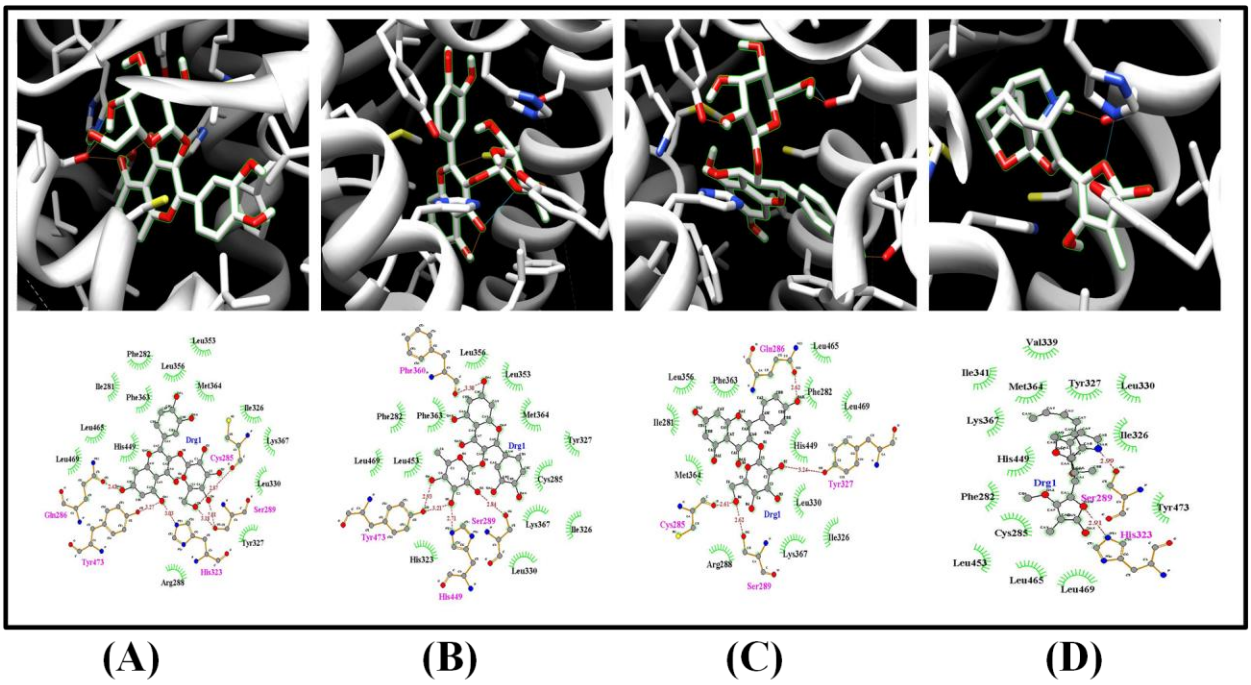

Figure 12: Interaction profile of the phytochemicals from with PPAR gamma: (A) – Asparagamine A; (B) – Isoquercitrin; (C) – Quercitrin; (D) – Leucopelargonidin 3-o-glucoside

3.3. CONCLUSION:

In adipogenesis, the *in silico* analysis was done in which the top 4 molecules were selected. Out of which the Asparagamine A and Leucopelargonidin 3-o-glucoside were also there. It can be estimated that these two can have a significant effect over the adipogenesis also, which can only be confirmed through the in vitro and vivo analysis. This in vitro and in vivo analysis can be done through the study of adipogenic differentiation for which optimization is required.

IV. SPECIAL TYPES OF CHRONIC ULCERS

Asparagus racemosus belongs to the family of Asparagaceae and is famous as Shatavari, is found in tropical and subtropical regions of Asia, Africa and Australia [117]. In traditional medicinal systems like Ayurveda, Unani and Siddha, this endangered plant has been reported to possess potential to treat variety of diseases and disorders. The plant is widely known for its excellent rejuvenating activity on female reproductive system. In addition ,the extracts from various parts of this plant is also well known to possess anti-ulcer, anti-bacterial, anti-depressant, anti-inflammatory, antiprotozoal, antiviral, antioxidant and anticancer properties [117-120]. Such a great variety of therapeutic usefulness of this plant is due to the wide variety of phytochemicals present in it. The major phytochemicals present in the *Asparagus racemosus* includes Shatavarins (I-IV), Idaein, Immunoside, Racemosides, Diosgenin, Sarasasapogenin and Asparagamine A etc. [117, 119-121]. Among these, Shatavarin IV has already been known to have anti-cancerous activity [122]. Keeping in view, the wide therapeutic activity of *Asparagus racemosus*, not much work has been done to attribute these therapeutic benefits to any specific phytochemical. Interestingly, when the structures of all the phytochemicals of this plant were evaluated, Asparagamine A, a polycyclic pyrrolizidine alkaloid, found to have a very unique cage like structure [123-124]. Though this unique structured Asparagamine A was isolated and characterized two decades ago by Sekine et.al., yet not much have been reported about its potential activities in the scientific literatures [123]. This compound has been reported to possess excellent antioxidant, anti-oxytocin, antitumor activities [124-126], but the effectiveness and efficacy of the compound was never evaluated over wide range of diseases against which asparagus racemosus has shown therapeutic benefits. In the present study, we have tried an In Silico approach to explore the therapeutic potentials of Asparagamine A over osteoporosis, AIDS, Tuberculosis, Cancer, Malaria, Leishmaniasis and Trypanosomiasis. The critical proteins which are considered to be essential for the development and progression of these diseases were isolated computationally and were docked with Asparagamine A using AutoDock4.2 tool (version 1.5.6).

4.1. MATERIALS AND METHODS

4.1.1. Protein structure retrieval:

The three dimensional crystal structures of target proteins were retrieved from Protein Data Bank (http://www.rcsb.org/pdb/). The proteins selected for targeting the diseases have been compiled in Table 1. Miscellaneous ligands and other hetero-atoms such as water, ions, etc. were removed from the protein models for active site predictions and further docking studies using Argus Lab Software.

4.1.2. Protein Active Site Predictions:

The active sites of target proteins were predicted by using CASTp Calculations (Computed Atlas of Surface Topography of proteins). Amongst the predicted site, the site having the catalytic amino acids was chosen for the docking of the ligand. The catalytic amino acids of the each protein were analyzed from UniProt (http://www.uniprot.org/).

4.1.3. Substrate selection:

The three dimensional structure of Asparagamine A was screened from KNApSAcK-3D database (http://knapsack3d.sakura.ne.jp/). The PDB structure of the ligand was deduced using PRODRG Server (davapc1.bioch.dundee.ac.uk/cgi-bin/prodrg). Ligand optimization and energy minimization was further done using Argus lab software. Apart from this, the three dimensional structures of standard inhibitors for all the aforesaid proteins were also deduced from PubChem database (http://pubchem.ncbi.nlm.nih.gov/) and were used as reference molecules.

4.1.4. Molecular Properties and Drug likeness:

The Asparagamine A was further examined for its drug likeness and molecular properties using FAF-Drug2 (http://mobyle.rpbs.univ-paris-diderot.fr/cgi-bin/portal.py?form=FAF Drugs#forms:: FAF- Drugs2) and PreADMET (http://preadmet.bmdrc.org/).

4.1.5. Molecular Docking:

The computational docking of Asparagamine A and standard inhibitors were performed into the active site of corresponding protein models using AutoDock4.2 software (version 1.5.6). While

docking, polar hydrogen's were added to protein models using the hydrogen's module and thereafter, Kollman united atom partial charges were assigned. Docking of ligand was carried out using Lamarckian Genetic Algorithm with standard docking protocol on the basis a population size of 150 randomly placed individuals; a maximum number of $2.5*10^7$ energy evaluations, a mutation rate of 0.02, a crossover rate of 0.80 and an elitism value of 1 [113]. Fifteen independent docking runs were carried out for each ligand and results were clustered according to the 1.0 Å rmsd criteria. The grid maps representing the proteins were calculated using autogrid and grid size was set to 60*60*60 points with grid spacing of 0.375 Å. The coordinate of the docked protein along with the ligand was visualized using UCSF chimera and LigPlot$^+$ [114].

4.2. RESULTS & DISCUSSIONS

Millions are being affected and millions are dying each year because of the diseases like AIDS, malaria, tuberculosis and Leishmaniasis**.** A number of drugs exist commercially that could be used for treatment of these diseases. But still the search of new lead molecules and drugs continues because of the side-effects posed by the existing drugs; emergence of the drug resistant forms of microorganisms and the need to develop drug with better efficacy and potency. The drugs developed against the above mentioned diseases are usually targeted towards some of the crucial proteins associated with the diseases or the causative microorganisms. The drugs and the corresponding proteins that they inhibit and hence have beneficial effect in these diseases are mentioned in the Table 15. In this study, Asparagamine A was targeted against those proteins to analyze its inhibitory effect over aforesaid diseases and the result was compared with the inhibitory efficiency of standard inhibitors.

Table 17: Potential Drug targets to target various diseases

Diseases	Proteins	Notations	Organism	PDB ID	Ref.
Tuberculosis	Mycolic Acid Cyclopropane Synthase	CmaA2	*Mycobacterium tuberculosis*	1KPI	[127]
	PKnB Kinase Domain	PKnB	*Mycobacterium tuberculosis*	1O6Y	[128]

HIV 1	HIV1 Protease	H1P	HIV	1AJV	[129]
Leishmaniasis	Trypanothione Reductase	LTR	*Leishmania infantum*	2JK6	[130]

ADME & Toxicity predictions were initially done to evaluate the pharmacokinetics and the toxicity of the phytochemicals/ligands. These predictions demonstrated that Asparagamine A did not have any mutagenicity and carcinogenicity. Asparagamine A was found to follow Lipinski's rule of five which allow the evaluation of pharmacokinetics of the drug including absorption, distribution, metabolism and excretion (ADME). The predicted percentage absorption of Asparagamine A through oral route was found to be 90.94%. High absorption of the drug allows it to achieve high concentration at the target site. Also the chemical was found to bind with plasma proteins weakly, making the majority of the unbound molecules available for diffusion, distribution and deposition across the body. The molecular properties as well as the three and two dimensional structure of Asparagamine A are mentioned in Table 17 and Figure 12 respectively.

Table 18: Molecular Properties of Asparagamine A

MOLECULAR PROPERTIES	
Molecular Weight	385.45
Log P	2.24
Log Sw	-3.44
tPSA	66.02
HB Donors	1
HB Acceptors	6
Lipinski's Violations	0
Solubility (mg\l)	12322.28
Oral Bioavailability (VEBER)	Good
Oral Bioavailability (EGAN)	Good
AMES Test	Non Mutagen

Carcinogenicity	Non Carcinogen
Human Intestinal Absorption (%)	90.947
In Vitro Plasma Protein Binding (%)	44.936

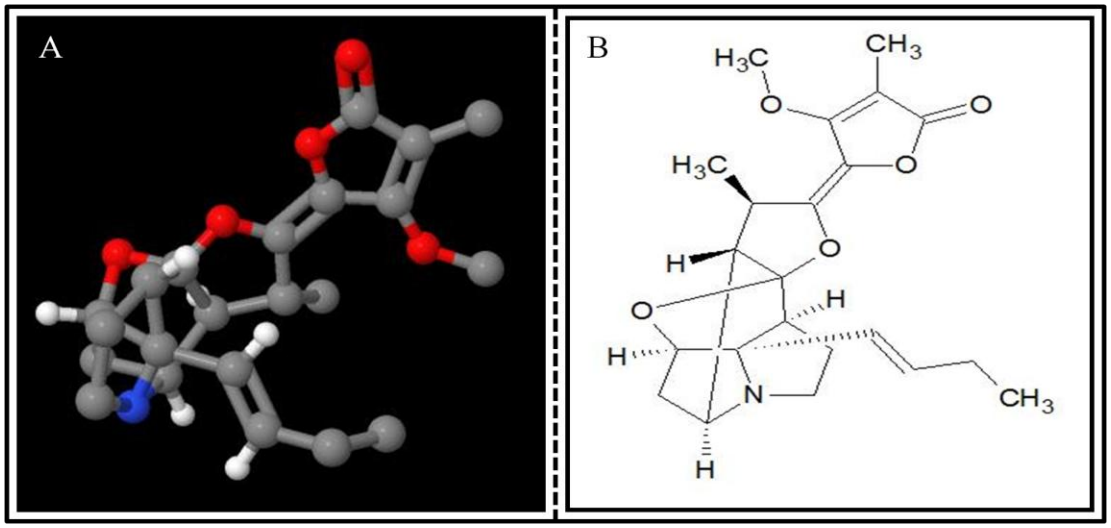

Figure 13: Three dimensional (A) and two dimensional (B) structure of Asparagamine A.

Molecular docking using the computational approach has been demonstrated as an effective methodology to analyze the interaction patterns of the ligand molecules with the proteins models. The interaction of drug with protein could bring some structural changes that may change or block its potential activity. A known fact is that the active site of protein plays a critical role in protein's activity and the computational designed drugs, usually targets these active sites. Docking analysis revealed that Asparagamine A possesses a very high affinity towards the HIV-1 proteases with estimated Ki values of 4.58 nM respectively. Both these proteins belong to the class of aspartic proteases and are usually targeted for drug designing against malaria and AIDS respectively [131-132]. HIV-1 protease catalyzes the proteolytic breakage of the polypeptide precursors into mature enzymes and structural proteins of the virus [133].

HIV infection has significantly contributed to worldwide re-emergence of tuberculosis incidences. With the development and evolution of the multi drug resistant (MDR) as extensively drug resistant (EDR) strains of *Mycobacterium tuberculosis* has drawn much of the attention towards the development of novel drugs [134-135]. In this regard, it is desired to design lead molecules that can simultaneously target both the diseases. Interestingly, Asparagamine A showed a binding energy of -9.48Kcal/mol and -8.54Kcal/mol towards CmaA2 and PKnB respectively; which have recently been identified as potential drug targets to combat tuberculosis [127-128]. CmaA2 is known to be a trans–cyclopropane synthase for both the methoxy- and keto- mycolates which are the major components of the cell envelope of *M. tuberculosis* and helps in the interaction of these bacteria with the human host [136]. PKnB is known as a functional kinase which gets autophosphorylated on serine/ threonine residues and is also capable of the phosphorylation of the myelin basic protein which is the main peptide substrate [137].

Another protein Trypanothione Reductase (TR) is unique to Leishmania and absent from mammalian cells, is considered as a potential drug target to combat Leishmaniasis [130, 138]. The Asparagamine A was found to have high affinity towards Trypanothione Reductases derived from both, *Leishmania infantum* (Ki: 17.75 nM) with estimated binding energies of -10.57 Kcal/mol.

It is highly desirable that a ligand must possess a high affinity for the protein to modulate the protein activity. The affinity of the ligand for the protein correlates with the binding energy of the protein ligand complex. Thus, lower the binding energy of the complex, higher the affinity of the ligand for the protein. The analysis of ligand's affinity towards the protein is insufficient to predict stable docking. Thus, it is essential to analyze the complete interaction profile of ligand with amino acid residues of the protein. The interactions that are usually accounted for in protein-ligand complex are hydrogen bonds and hydrophobic interactions. The presence of these hydrogen bonds and hydrophobic interactions increases the stability of protein ligand complex. In this regard, the probable hydrogen bonds and hydrophobic interactions formed between proteins and Asparagamine A was illustrated through Chimera (Table 18) and LigPlot^{+} (Table 19). The interaction can be viewed in Figure 13.

Table 19: Binding Interactions of Asparagamine A – Docking and Chimera Analysis:

Proteins	**Minimum Binding Energy (Kcal/mol)**	**Ki (nM)**	**Hydrogen Bonds**	**Interacting Amino Acids**

CmaA2	-9.48	111.94	0	-
PKnB	-8.54	553.05	3	Lys40 (2), Asp156
H1P	-11.38	4.58	2	Ile50, Asp128
LTR	-10.57	17.75	6	Thr51, Asp327 (3), Met333, Thr335,

Table 20: Molecular Interactions of Asparagamine A – LigPlot^{+} Analysis:

Proteins	**Interacting Amino Acids via**	
	Hydrogen Bonds	**Hydrophobic Interactions**
CmaA2	-	Tyr24, Tyr41, Gly145, Ile184, Ile210, Leu211, Phe215, Gly218, Leu220, Tyr247, Trp254, Tyr280,Cys284, Phe288
PKnB	Lys40, Asp138, Asp156	Phe19, Gly20, Met22, Ser23, Val25, Met155, Gly158, Thr159
H1P	Asp 124, Asp 128, Ile50	Asp25, Gly27,Ala28,Gly48, Gly49, Gly126, Ala127, Asp129, Val131, Ile146, Gly147, Ile149,Pro180,Val181, Ile183
LTR	Asp327 (2), Thr335	Gly13, Ser14, Gly50, Thr51, Cys52, Gly56, Cys57, Ala159, Gly161, Ser162, Tyr198, Arg287, Gly326, Met333, Leu334

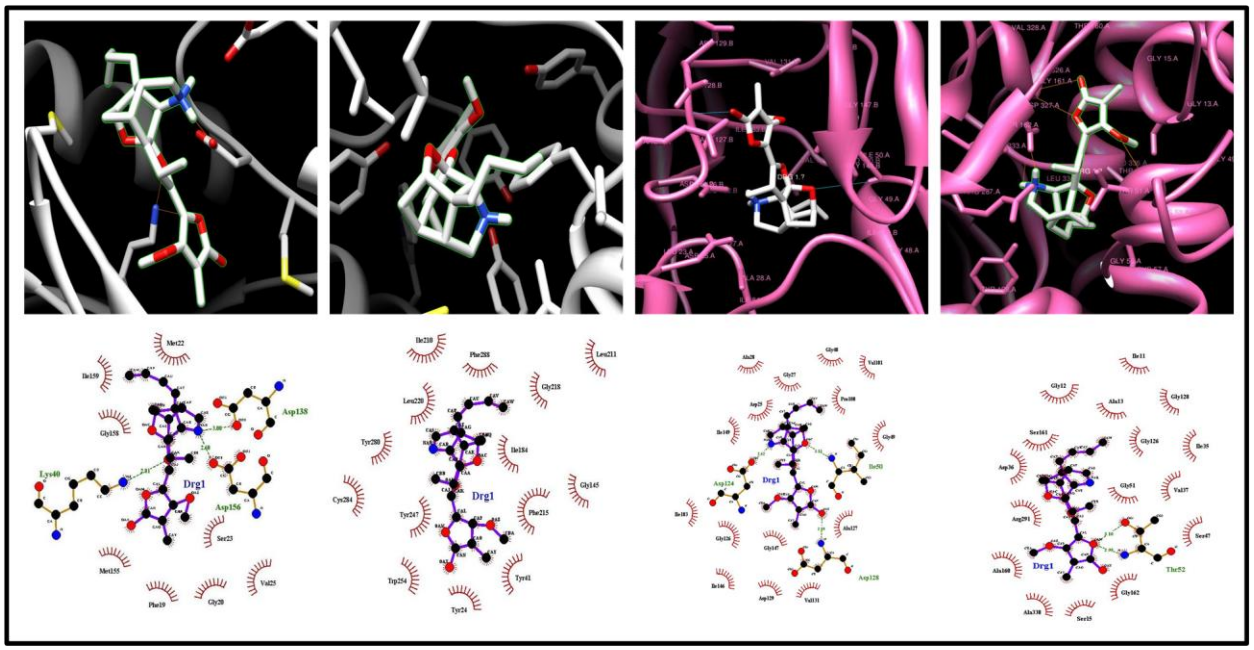

Figure 14: Molecular interactions of Asparagamine A- UCSF Chimera & LigPlot^{+}: (A) - CmaA2 (Tuberculosis); (B) - PKnB (Tuberculosis); (C) – H1P (AIDS); (D) – LTR (Leishmaniasis)

A comparative analysis of the binding affinity of Asparagamine A and the reference molecules towards the corresponding proteins suggested that the alkaloid Asparagamine A could be developed into potential therapeutic agent for the treatment of many diseases (Table 20 and 21). The analogues of Asparagamine A could also be developed for the improvement of its specificity and affinity towards a protein target. The chemical synthesis of Asparagamine A was reported by Brüggemann M. *et.al*., also makes it a suitable candidate for much desirable mass scale production of the ligand and its analogues [139].

Table 21: Binding Energy of Reference Inhibitors (Standard drugs):

Proteins	**Inhibitors**	**Minimum Binding Energy (Kcal/mol)**	**Ki (nM)**
CmaA2	Thioacetazone [127]	-6.26	26000
PKnB	2,4-Dichloroquinazoline [128]	-4.75	330000

H1P	Indinavir [129]	-11.17	6
	Amprenavir [129]	-9.62	89
LTR	Ebsulfur [140]	-6.96	7970

Table 22: Comparison between the standard drugs with Asparagamine A

Proteins	**Inhibitors**	**Ki (nM) [Standard drugs]**	**Ki (nM) [Asparagamine A]**
CmaA2	Thioacetazone	26000	111.94
PKnB	2,4-Dichloroquinazoline	330000	553.05
H1P	Indinavir	6	4.58
	Amprenavir	89	4.58
LTR	Ebsulfur	7970	17.75

4.3. CONCLUSION

The complete study was conducted *in silico* to explore the therapeutic potentials of the ligand Asparagamine A derived from *A. racemosus*. The overall analysis suggests that Asparagamine A shows a higher affinity towards the critical proteins that are generally targeted to combat aforesaid mentioned diseases. The study provides a clue for the development of a new lead that could be used for the prevention or cure of multiple diseases. Further, *In vitro* and *In vivo* validation of aforesaid therapeutic potentials of Asparagamine A is required.

V. CHRONIC INFLAMMATION

Wound healing initially begins with the inflammation in which the blood vessels dilate and neutrophils infiltrate into the injury site. Macrophages are released which release inflammatory cells as well as more of macrophages. These inflammatory cells cause inflammation in the area of the injury. Apart from the inflammation due to these cells, the reasons mentioned in all the chapters, involve the development of severe (chronic) inflammation and persistence of the wounds for a long period of time.

Inflammation itself is of two types: Acute and chronic inflammation. On one side, acute inflammation is there which is quite regulated but chronic inflammation is completely dysregulated. Inflammation usually begins in a controlled manner so as to protect the body from the infection but it can change its path to an unregulated one. This leads to the chronic phase of inflammation. Normal process of wound healing continues but the cell composition changes. Chronic inflammation is one of a major problem being faced today. This leads to delayed healing of severe wounds, diabetes, ulcers [141-142]. Apart from this, chronic inflammation also affects the arteries and the blood vessels which can cause Heart attack, Cancer, etc [143-144].

A major polyphenol phytochemical present in turmeric, which is known as Curcumin ($C_{21}H_{20}O_6$), is a yellow pigment from Curcuma longa. This is used as the food colouring agent and also used in cosmetics and in medical preparations. Therapeutic potentials of curcumin include majorly its antioxidant, anti – inflammatory properties [145]. The mechanism of its properties includes the down regulation of the role played by major enzymes, namely cyclooxygenase -2 (COX-2), nitric oxide synthase (iNOS). Along with this, there is a decrease in the release of Tumor necrosis factor – alpha (TNF-α), interleukins (IL) and major inflammatory cytokines. Curcumin is known to subdue the activity of nuclear factor kappa beta (NF-κβ) which in turn inhibits COX-2 and iNOS. This NF- κβ is a transcription factor which takes part in the regulation of inflammation, cellular proliferation, and tumorogenic behavior [146-147].

Curcumin is important not only in inflammation, but also in the many chronic pathological diseases like cancer, atherosclerosis, etc. Curcumin shows its anti- cancerous activity by affecting the cell cycle and mutagenic pathways, etc [148]. The down regulation of the transcription factors, interleukins related to the disorder lead to the anti – proliferation of the tumorogenic cells [149].

5.1. MATERIAL AND METHODS:

5.1.1. Drug release kinetics:

The polymer – ECM composite films were used for the drug release analysis by incorporating curcumin inside the films. The films were kept in a tube whose cap was covered with dialysis membrane and the whole system was dipped in PBS. The fixed volume of PBS was taken at regular interval of time of 15 min, 30 min, 45 min, 1 hr, 2 hr, 3 hr, 4 hr, 5 hr, 6 hr, 8 hr, 12 hr, 24 hr, 48 hr, 72 hr, 96 hr, 120 hr, and 144 hr. The volume was made constant by replacing it with fresh PBS. The absorbance of all the samples was taken at 420 nm [150].

Statistical Analysis:

Each experiment was performed in triplicates. All the results were mentioned as the average (mean) ± S.D. Statistical analysis of all the quantitative data was done using one – way ANOVA through IBM SPSS Statistics 20.0. The results of all the samples were compared at 95% of confidence level. The results with p – value equal or less than 0.05 were considered to be statistically significant.

RESULTS AND DISCUSSION:

Drug release kinetics:

The release of drug was recorded at the regular interval of time by measuring the absorbance at 570 nm. A comparative slow release was observed in the composites when compared with the chitosan or alginate control samples. This may be due to the cross-linking of the curcumin with the ECM. This is even better if the films are to be used for the wound healing purpose.

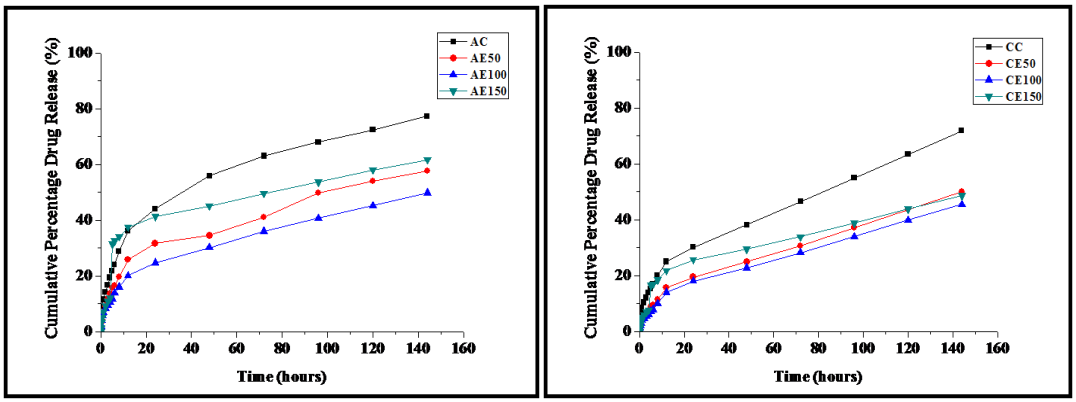

Figure 15. Drug release kinetics in Chitosan – Extracellular matrix and Alginate – Extracellular matrix composite films

The main purpose of adding curcumin into the prepared film was to prepare such a scaffold which has a drug which act majorly against inflammation due major diseases. Curcumin being a phytochemical available in pure form was taken. The comparison among different films was done after incorporating the phytochemical. It was good to observe that there was a very slow and steady release of drug from the film as compared to the control. It may be due to some crosslinking with the extracellular matrix which is making it to release out slowly.

Since Curcumin also inhibit adipogenesis, so it cannot be used for the deep wounds where there is complete loss of adipose tissue as those effected regions need the restoration of adipose tissue. The wounds which are superficial and need re-epithelialization rather than adipogenesis, there these films along with curcumin can be efficiently used.

CONCLUSION:

The biological and medicinal property of curcumin makes it beneficial for the treatment of the chronic wounds. The films prepared were tested for their role in the superficial burns by incorporating curcumin in it. Curcumin, added to the films made the film very stiff and strong, that is, with high mechanical strength. This is due to the fact that curcumin cross-links with ECM and polymer, thus causing slow release of drug.

REFERENCES

[1] T. Kondo and Y. Ishida, "Molecular pathology of wound healing," *Forensic science international,* vol. 203, pp. 93-98, 2010.

[2] I. George Broughton, J. E. Janis, and C. E. Attinger, "Wound healing: an overview," *Plastic and reconstructive surgery,* vol. 117, pp. 1e-S-32e-S, 2006.

[3] D. Kelly Wallin and D. Gerit Mulder, "REGENERATIVE MATERIALS THAT FACILITATE WOUND HEALING."

[4] R. F. Diegelmann and M. C. Evans, "Wound healing: an overview of acute, fibrotic and delayed healing," *Front Biosci,* vol. 9, pp. 283-289, 2004.

[5] R. Goldman, "Growth factors and chronic wound healing: past, present, and future," *Advances in skin & wound care,* vol. 17, pp. 24-35, 2004.

[6] M. J. P. Hodde and C. E. Johnson, "Extracellular matrix as a strategy for treating chronic wounds," *American journal of clinical dermatology,* vol. 8, pp. 61-66, 2007.

[7] B. A. Schmidt and V. Horsley, "Intradermal adipocytes mediate fibroblast recruitment during skin wound healing," *Development,* vol. 140, pp. 1517-1527, 2013.

[8] W. A. Marston, J. Hanft, P. Norwood, and R. Pollak, "The Efficacy and Safety of Dermagraft in Improving the Healing of Chronic Diabetic Foot Ulcers Results of a prospective randomized trial," *Diabetes Care,* vol. 26, pp. 1701-1705, 2003.

[9] L. Zaulyanov and R. S. Kirsner, "A review of a bi-layered living cell treatment (Apligraf®) in the treatment of venous leg ulcers and diabetic foot ulcers," *Clinical interventions in aging,* vol. 2, p. 93, 2007.

[10] S. Bale, D. Squires, T. Varnon, A. Walker, M. Benbow, and K. Harding, "A comparison of two dressings in pressure sore management," *Journal of wound care,* vol. 6, pp. 463-466, 1997.

[11] D. Berry, S. Bale, and K. Harding, "Dressings for treating cavity wounds," *Journal of wound care,* vol. 5, pp. 10-17, 1996.

[12] J. Macfie and M. J. McMahon, "The management of the open perineal wound using a foam elastomer dressing: a prospective clinical trial," *British Journal of Surgery,* vol. 67, pp. 85-89, 1980.

[13] S. Matzen, A. Peschardt, and B. Alsbjørn, "A new amorphous hydrocolloid for the treatment of pressure sores: a randomised controlled study," *Scandinavian journal of plastic and reconstructive surgery and hand surgery,* vol. 33, pp. 13-15, 1999.

[14] A. DeFranzo, L. Argenta, M. Marks, J. Molnar, L. David, L. Webb, W. Ward, and R. Teasdall, "The use of vacuum-assisted closure therapy for the treatment of lower-extremity wounds with exposed bone," *Plastic and reconstructive surgery,* vol. 108, pp. 1184-1191, 2001.

[15] T. Velnar, T. Bailey, and V. Smrkolj, "The wound healing process: an overview of the cellular and molecular mechanisms," *Journal of International Medical Research,* vol. 37, pp. 1528-1542, 2009.

[16] S. Guo and L. A. DiPietro, "Factors affecting wound healing," *Journal of dental research,* vol. 89, pp. 219-229, 2010.

[17] C. Patrick, "Tissue engineering strategies for adipose tissue repair," *The Anatomical Record,* vol. 263, pp. 361-366, 2001.

[18] L. Hong, I. A. Peptan, A. Colpan, and J. L. Daw, "Adipose tissue engineering by human adipose-derived stromal cells," *Cells Tissues Organs,* vol. 183, pp. 133-140, 2006.

[19] E. Billings Jr and J. W. May Jr, "Historical review and present status of free fat graft autotransplantation in plastic and reconstructive surgery," *Plastic and reconstructive surgery,* vol. 83, pp. 368-381, 1989.

[20] W. R. Beahm E, Patrickjr C, "Progress in adipose tissue construct development," *Clinics in Plastic Surgery,* vol. 30, pp. 547-58, 2003.

[21] J. H. Choi, J. M. Gimble, K. Lee, K. G. Marra, J. P. Rubin, J. J. Yoo, G. Vunjak-Novakovic, and D. L. Kaplan, "Adipose tissue engineering for soft tissue regeneration," *Tissue Engineering Part B: Reviews,* vol. 16, pp. 413-426, 2010.

[22] A. S. Halim, T. L. Khoo, and S. J. M. Yussof, "Biologic and synthetic skin substitutes: An overview," *Indian journal of plastic surgery: official publication of the Association of Plastic Surgeons of India,* vol. 43, p. S23, 2010.

[23] P. M. Crapo, T. W. Gilbert, and S. F. Badylak, "An overview of tissue and whole organ decellularization processes," *Biomaterials*, vol. 32, pp. 3233-3243, 2011.

[24] D. J. Rosario, G. C. Reilly, E. Ali Salah, M. Glover, A. J. Bullock, and S. MacNeil, "Decellularization and sterilization of porcine urinary bladder matrix for tissue engineering in the lower urinary tract," 2008.

[25] L. Sorokin, "The impact of the extracellular matrix on inflammation," *Nature Reviews Immunology*, vol. 10, pp. 712-723, 2010.

[26] R. Cartier, I. Brunette, K. Hashimoto, W. Bourne, and H. Schaff, "Angiogenic factor: a possible mechanism for neovascularization produced by omental pedicles," *The Journal of thoracic and cardiovascular surgery*, vol. 99, p. 264, 1990.

[27] R. Saltz, R. Stowers, M. Smith, and T. R. Gadacz, "Laparoscopically harvested omental free flap to cover a large soft tissue defect," *Annals of surgery*, vol. 217, p. 542, 1993.

[28] P. Micheau, "The greater omentum. Its role in reconstructive plastic surgery," in *Annales de chirurgie plastique et esthetique*, 1995, pp. 192-207.

[29] M. Ignjatović, S. Pervulov, V. Ćuk, Z. Kostić, and L. Minić, "Early angiogenic capabilities of the transposed omental flap after omentomyelopexy," *Acta chirurgica iugoslavica*, vol. 48, pp. 41-43, 2001.

[30] S. S. Costa, R. M. Blotta, M. B. Mariano, L. Meurer, and M. I. A. Edelweiss, "Laparoscopic treatment of Poland's syndrome using the omentum flap technique," *Clinics*, vol. 65, pp. 401-406, 2010.

[31] A. Porzionato, M. Sfriso, V. Macchi, A. Rambaldo, G. Lago, L. Lancerotto, V. Vindigni, and R. De Caro, "Decellularized omentum as novel biologic scaffold for reconstructive surgery and regenerative medicine," *European journal of histochemistry: EJH*, vol. 57, 2013.

[32] R. K. Keith Harding, Daniel Lee, Gerit Mulder, Thomas Serena., "Acellular Matrices for the treatment of Wounds," *Wounds International* 2011.

[33] D. Gibson, "MMPs Made Easy. Wounds International; 1 (1)," ed, 2009.

[34] J. Liao, X. Guo, K. J. Grande-Allen, F. K. Kasper, and A. G. Mikos, "Bioactive polymer/extracellular matrix scaffolds fabricated with a flow perfusion bioreactor for cartilage tissue engineering," *Biomaterials*, vol. 31, pp. 8911-8920, 2010.

[35] A. K. Azad, N. Sermsintham, S. Chandrkrachang, and W. F. Stevens, "Chitosan membrane as a wound healing dressing: Characterization and clinical application," *Journal of Biomedical Materials Research Part B: Applied Biomaterials,* vol. 69, pp. 216-222, 2004.

[36] S.-Y. Ong, J. Wu, S. M. Moochhala, M.-H. Tan, and J. Lu, "Development of a chitosan-based wound dressing with improved hemostatic and antimicrobial properties," *Biomaterials,* vol. 29, pp. 4323-4332, 2008.

[37] T. Dai, M. Tanaka, Y.-Y. Huang, and M. R. Hamblin, "Chitosan preparations for wounds and burns: antimicrobial and wound-healing effects," 2011.

[38] H. Ueno, T. Mori, and T. Fujinaga, "Topical formulations and wound healing applications of chitosan," *Advanced drug delivery reviews,* vol. 52, pp. 105-115, 2001.

[39] R. Jayakumar, M. Prabaharan, P. Sudheesh Kumar, S. Nair, and H. Tamura, "Biomaterials based on chitin and chitosan in wound dressing applications," *Biotechnology advances,* vol. 29, pp. 322-337, 2011.

[40] D. Archana, J. Dutta, and P. Dutta, "Evaluation of chitosan nano dressing for wound healing: Characterization, in vitro and in vivo studies," *International journal of biological macromolecules,* vol. 57, pp. 193-203, 2013.

[41] M. P. Ribeiro, A. Espiga, D. Silva, P. Baptista, J. Henriques, C. Ferreira, J. C. Silva, J. P. Borges, E. Pires, and P. Chaves, "Development of a new chitosan hydrogel for wound dressing," *Wound Repair and Regeneration,* vol. 17, pp. 817-824, 2009.

[42] I. A. Alsarra, "Chitosan topical gel formulation in the management of burn wounds," *International journal of biological macromolecules,* vol. 45, pp. 16-21, 2009.

[43] Y. Zhou, H. Yang, X. Liu, J. Mao, S. Gu, and W. Xu, "Potential of quaternization-functionalized chitosan fiber for wound dressing," *International journal of biological macromolecules,* vol. 52, pp. 327-332, 2013.

[44] Y. Zhu, T. Liu, K. Song, B. Jiang, X. Ma, and Z. Cui, "Collagen–chitosan polymer as a scaffold for the proliferation of human adipose tissue-derived stem cells," *Journal of Materials Science: Materials in Medicine,* vol. 20, pp. 799-808, 2009.

[45] S. P. Tsai, C. Y. Hsieh, C. Y. Hsieh, D. M. Wang, L. L. H. Huang, J. Y. Lai, and H. J. Hsieh, "Preparation and cell compatibility evaluation of chitosan/collagen composite

scaffolds using amino acids as crosslinking bridges," *Journal of applied polymer science*, vol. 105, pp. 1774-1785, 2007.

[46] Z. Gu, H. Xie, C. Huang, L. Li, and X. Yu, "Preparation of chitosan/silk fibroin blending membrane fixed with alginate dialdehyde for wound dressing," *International journal of biological macromolecules*, vol. 58, pp. 121-126, 2013.

[47] H. B. TVL, M. Vidyavathi, and T. Sastry, "Preparation and evaluation of ciprofloxacin loaded chitosan-gelatin composite films for wound healing activity," *International Journal of Drug Delivery*, vol. 2, 2011.

[48] H. B. TVL, M. Vidyavathi, K. Kavitha, and T. Sastry, "Preparation and Evaluation of Chitosan-Gelatin Composite Films for Wound Healing Activity."

[49] N. Van Cuong, N. Van Boi, and M.-F. Hsieh, "Curcumin - loaded Chitosan/ Gelatin composite sponge for wound healing application."

[50] J. Venkatesan and S.-K. Kim, "Chitosan composites for bone tissue engineering—An overview," *Marine drugs*, vol. 8, pp. 2252-2266, 2010.

[51] G. Kratz, C. Arnander, J. Swedenborg, M. Back, C. Falk, I. Gouda, and O. Larm, "Heparin-chitosan complexes stimulate wound healing in human skin," *Scandinavian Journal of Plastic and Reconstructive Surgery and Hand Surgery*, vol. 31, pp. 119-123, 1997.

[52] L. Chen, C.-y. Tang, N.-y. Ning, C.-y. Wang, Q. Fu, and Q. Zhang, "Preparation and properties of chitosan/lignin composite films," *Chinese Journal of Polymer Science*, vol. 27, pp. 739-746, 2009.

[53] X. Li, K. Nan, L. Li, Z. Zhang, and H. Chen, "In vivo evaluation of curcumin nanoformulation loaded methoxy poly (ethylene glycol)-graft-chitosan composite film for wound healing application," *Carbohydrate Polymers*, vol. 88, pp. 84-90, 2012.

[54] M. M. Stevens, H. F. Qanadilo, R. Langer, and V. Prasad Shastri, "A rapid-curing alginate gel system: utility in periosteum-derived cartilage tissue engineering," *Biomaterials*, vol. 25, pp. 887-894, 2004.

[55] C. K. Kuo and P. X. Ma, "Ionically crosslinked alginate hydrogels as scaffolds for tissue engineering: part 1. Structure, gelation rate and mechanical properties," *Biomaterials*, vol. 22, pp. 511-521, 2001.

[56] M. Dai, X. Zheng, X. Xu, X. Kong, X. Li, G. Guo, F. Luo, X. Zhao, Y. Q. Wei, and Z. Qian, "Chitosan-alginate sponge: preparation and application in curcumin delivery for dermal wound healing in rat," *BioMed Research International,* vol. 2009, 2009.

[57] A. D. Augst, H. J. Kong, and D. J. Mooney, "Alginate hydrogels as biomaterials," *Macromolecular bioscience,* vol. 6, pp. 623-633, 2006.

[58] Y. Suzuki, Y. Nishimura, M. Tanihara, K. Suzuki, A. K. Kitahara, Y. Yamawaki, T. Nakamura, Y. Shimizu, and Y. Kakimaru, "Development of alginate gel dressing," *Journal of Artificial Organs,* vol. 1, pp. 28-32, 1998.

[59] Y. C. Choi, J. S. Choi, B. S. Kim, J. D. Kim, H. I. Yoon, and Y. W. Cho, "Decellularized extracellular matrix derived from porcine adipose tissue as a xenogeneic biomaterial for tissue engineering," *Tissue Engineering Part C: Methods,* vol. 18, pp. 866-876, 2012.

[60] M. Kouchak, A. Ameri, B. Naseri, and S. Kargar Boldaji, "Chitosan and polyvinyl alcohol composite films containing nitrofurazone: preparation and evaluation," *Iranian Journal of Basic Medical Sciences,* vol. 17, pp. 14-20, 2014.

[61] S. Zivanovic, J. Li, P. M. Davidson, and K. Kit, "Physical, mechanical, and antibacterial properties of chitosan/PEO blend films," *Biomacromolecules,* vol. 8, pp. 1505-1510, 2007.

[62] P. Gentile, M. Mattioli-Belmonte, V. Chiono, C. Ferretti, F. Baino, C. Tonda-Turo, C. Vitale-Brovarone, I. Pashkuleva, R. L. Reis, and G. Ciardelli, "Bioactive glass/polymer composite scaffolds mimicking bone tissue," *Journal of Biomedical Materials Research Part A,* vol. 100, pp. 2654-2667, 2012.

[63] S. Patricia Miranda, O. Garnica, V. Lara-Sagahon, and G. Cárdenas, "Water vapor permeability and mechanical properties of chitosan composite films," *Journal of the Chilean Chemical Society,* vol. 49, pp. 173-178, 2004.

[64] H.-M. Wang, Y.-T. Chou, Z.-H. Wen, Z.-R. Wang, C.-H. Chen, and M.-L. Ho, "Novel biodegradable porous scaffold applied to skin regeneration," *PloS one,* vol. 8, p. e56330, 2013.

[65] K. Pal and S. Pal, "Development of porous hydroxyapatite scaffolds," *Materials and manufacturing processes,* vol. 21, pp. 325-328, 2006.

[66] P. Wang, J. Liu, and T. Zhang, "In Vitro Biocompatibility of Electrospun Chitosan/Collagen Scaffold," *Journal of Nanomaterials,* vol. 2013, 2013.

[67] K. Girhepunje, P. R. Krishnapiillai, H. Gevariya, and N. Thirumoorthy, "Celecoxib loaded microbeads: A targeted drug delivery for colorectal cancer," *Int J Chem Pharm Res*, vol. 2, pp. 46-55, 2010.

[68] C. Sussman and B. M. Bates-Jensen, *Wound care: a collaborative practice manual*: Lippincott Williams & Wilkins, 2007.

[69] R. L. K. J. Autian, Z. Oser, E.Martin (Eds, *Polymer Science and Technology,* vol. Vol 8, pp. 181-195, 1975.

[70] X.-H. Qu, Q. Wu, and G.-Q. Chen, "In vitro study on hemocompatibility and cytocompatibility of poly (3-hydroxybutyrate-co-3-hydroxyhexanoate)," *Journal of Biomaterials Science, Polymer Edition,* vol. 17, pp. 1107-1121, 2006.

[71] B. Li, C.-L. Shan, Q. Zhou, Y. Fang, Y.-L. Wang, F. Xu, L.-R. Han, M. Ibrahim, L.-B. Guo, and G.-L. Xie, "Synthesis, characterization, and antibacterial activity of cross-linked chitosan-glutaraldehyde," *Marine drugs,* vol. 11, pp. 1534-1552, 2013.

[72] K. Belbachir, R. Noreen, G. Gouspillou, and C. Petibois, "Collagen types analysis and differentiation by FTIR spectroscopy," *Analytical and bioanalytical chemistry,* vol. 395, pp. 829-837, 2009.

[73] M. AbdElhady, "Preparation and characterization of chitosan/zinc oxide nanoparticles for imparting antimicrobial and UV protection to cotton fabric," *International Journal of Carbohydrate Chemistry,* vol. 2012, 2012.

[74] P. Sundarrajan, P. Eswaran, A. Marimuthu, L. B. Subhadra, and P. Kannaiyan, "One Pot Synthesis and Characterization of Alginate Stabilized Semiconductor Nanoparticles," *Bulletin of the Korean Chemical Society,* vol. 33, pp. 3218-3224, 2012.

[75] M. W. Laschke, Y. Harder, M. Amon, I. Martin, J. Farhadi, A. Ring, N. Torio-Padron, R. Schramm, M. Rücker, and D. Junker, "Angiogenesis in tissue engineering: breathing life into constructed tissue substitutes," *Tissue Eng,* vol. 12, pp. 2093-2104, 2006.

[76] J. Dai and A. Rabie, "VEGF: an essential mediator of both angiogenesis and endochondral ossification," *J Dent Res,* vol. 86, pp. 937-950, 2007.

[77] P. Carmeliet, "Angiogenesis in health and disease," *Nat med,* vol. 9, pp. 653-660, 2003.

[78] P. J. Polverini, "The pathophysiology of angiogenesis," *Crit Rev Oral Biol M,* vol. 6, pp. 230-247, 1995.

[79] A.-K. Olsson, A. Dimberg, J. Kreuger, and L. Claesson-Welsh, "VEGF receptor signalling? In control of vascular function," *Nat Rev Mol Cell Biol,* vol. 7, pp. 359-371, 2006.

[80] S. Saha, M. K. Islam, J. A. Shilpi, and S. Hasan, "Inhibition of VEGF: a novel mechanism to control angiogenesis by Withania somnifera's key metabolite Withaferin A," *In Silico Pharmacol,* vol. 1, pp. 1-9, 2013.

[81] O. Kadioglu, E. Seo, and T. Efferth, "Targeting Angiogenesis By Phytochemicals," *Med Aromat Plants,* vol. 2, pp. 1-8, 2013.

[82] R. Schindler and R. Mentlein, "Flavonoids and vitamin E reduce the release of the angiogenic peptide vascular endothelial growth factor from human tumor cells," *J Nutr,* vol. 136, pp. 1477-1482, 2006.

[83] E. Bagli, M. Stefaniotou, L. Morbidelli, M. Ziche, K. Psillas, C. Murphy, and T. Fotsis, "Luteolin inhibits vascular endothelial growth factor-induced angiogenesis; inhibition of endothelial cell survival and proliferation by targeting phosphatidylinositol 3′-kinase activity," *Cancer Res,* vol. 64, pp. 7936-7946, 2004.

[84] P. Anand, S. G. Thomas, A. B. Kunnumakkara, C. Sundaram, K. B. Harikumar, B. Sung, S. T. Tharakan, K. Misra, I. K. Priyadarsini, and K. N. Rajasekharan, "Biological activities of curcumin and its analogues (Congeners) made by man and Mother Nature," *Biochem Pharm,* vol. 76, pp. 1590-1611, 2008.

[85] F.-L. Hsu, I.-M. Liu, D.-H. Kuo, W.-C. Chen, H.-C. Su, and J.-T. Cheng, "Antihyperglycemic effect of puerarin in streptozotocin-induced diabetic rats," *J Nat Prod,* vol. 66, pp. 788-792, 2003.

[86] Y. Tanwar, S. Goyal, and K. Ramawat, "Hypolipidemic effects of tubers of Indian kudzu (Pueraria tuberosa)," *J Herb Med Toxicol,* vol. 2, pp. 21-25, 2008.

[87] R. Gupta, R. Sharma, A. Sharma, R. Choudhary, A. Bhatnager, and Y. Joshi, "Antifertility Effects of Pueraria tuberosa. Root Extract in Male Rats," *Pharm Biol,* vol. 42, pp. 603-609, 2005.

[88] S. Shukla, S. Jonathan, and A. Sharma, "Protective action of butanolic extract of Pueraria tuberosa DC. against carbon tetrachloride induced hepatotoxicity in adult rats," *Phytother Res,* vol. 10, pp. 608-609, 1996.

[89] R. A. Khan, P. K. Agrawal, and R. S. Kapil, "Puetuberosanol, an epoxychalcanol from *Pueraria tuberosa*," *Phytochemistry,* vol. 42, pp. 243-244, 1996.

[90] B. S. Joshi and V. N. Kamat, "Tuberosin, a new pterocarpan from Pueraria tuberosa DC," *J Chem Soc, Perkin Trans 1,* pp. 907-911, 1973.

[91] A. Koul and G. Sumbali, "Detection of zearalenone, zearalenol and deoxynivalenol from medicinally important dried rhizomes and root tubers," *Afr J Biotechnol,* vol. 7, pp. 4136-4139, 2008.

[92] M. Sharma, A. Sharma, and A. Kumar, "Ethnopharmacological importance of Asparagus racemosus: A review," *Journal of Pharmaceutical and Biomedical Sciences (JPBMS),* vol. 6, 2011.

[93] B. Joseph and S. J. Raj, "PHYTOPHARMACOLOGICAL AND PHYTOCHEMICAL PROPERTIES OF THREE FICUS SPECIES-AN OVERVIEW," *International Journal of Pharma & Bio Sciences,* vol. 1, 2010.

[94] B. Joseph and S. J. Raj, "AN OVERVIEW-FICUS BENGALENSIS LINN," *International Journal of Pharmaceutical Sciences Review & Research,* vol. 6, 2011.

[95] G. M. Morris, D. S. Goodsell, R. S. Halliday, R. Huey, W. E. Hart, R. K. Belew, and A. J. Olson, "Automated docking using a Lamarckian genetic algorithm and an empirical binding free energy function," *J Comput Chem,* vol. 19, pp. 1639-1662, 1998.

[96] E. F. Pettersen, T. D. Goddard, C. C. Huang, G. S. Couch, D. M. Greenblatt, E. C. Meng, and T. E. Ferrin, "UCSF Chimera—a visualization system for exploratory research and analysis," *J Comput Chem,* vol. 25, pp. 1605-1612, 2004.

[97] R. A. Laskowski and M. B. Swindells, "LigPlot+: multiple ligand–protein interaction diagrams for drug discovery," *J Chem Inf Model,* vol. 51, pp. 2778-2786, 2011.

[98] J. A. Wani, R. N. Achur, and R. Nema, "Phytochemical screening and aphrodisiac activity of Asparagus racemosus," *studies,* vol. 8, p. 9, 2011.

[99] A. Wadood, M. Ghufran, S. Jamal, M. Naeem, and A. Khan, "Phytochemical Analysis of Medicinal Plants Occurring in Local Area of Mardan," *Biochem Anal Biochem,* vol. 2, pp. 2161-1009.100014, 2013.

[100] G. Neufeld, T. Cohen, S. Gengrinovitch, and Z. Poltorak, "Vascular endothelial growth factor (VEGF) and its receptors," *FASEB J,* vol. 13, pp. 9-22, 1999.

[101] R. Roskoski Jr, "VEGF receptor protein–tyrosine kinases: structure and regulation," *Biochem Biophys Res Commun,* vol. 375, pp. 287-291, 2008.

[102] J. Solowiej, S. Bergqvist, M. A. McTigue, T. Marrone, T. Quenzer, M. Cobbs, K. Ryan, R. S. Kania, W. Diehl, and B. W. Murray, "Characterizing the effects of the juxtamembrane domain on vascular endothelial growth factor receptor-2 enzymatic activity, autophosphorylation, and inhibition by axitinib," *Biochemistry,* vol. 48, pp. 7019-7031, 2009.

[103] E.-J. Seo, V. Kuete, O. Kadioglu, B. Krusche, S. Schröder, H. J. Greten, J. Arend, I.-S. Lee, and T. Efferth, "Antiangiogenic activity and pharmacogenomics of medicinal plants from traditional Korean medicine," *Evid Based Complement Alternat Med,* vol. 2013, pp. 1-13, 2013.

[104] Y. Oguro, N. Miyamoto, K. Okada, T. Takagi, H. Iwata, Y. Awazu, H. Miki, A. Hori, K. Kamiyama, and S. Imamura, "Design, synthesis, and evaluation of 5-methyl-4-phenoxy-5H-pyrrolo [3, 2-d] pyrimidine derivatives: Novel VEGFR2 kinase inhibitors binding to inactive kinase conformation," *Bioorg Med Chem,* vol. 18, pp. 7260-7273, 2010.

[105] R. A. Khan and R. S. Kapil, "A facile synthesis of biogenetic precursor, puerarone, isolated from Pueraria sp," *J Heterocyclic Chem,* vol. 38, pp. 1007-1009, 2001.

[106] N. Pandey and Y. B. Tripathi, "Antioxidant activity of tuberosin isolated from Pueraria tuberose Linn," *J Inflamm,* vol. 7, pp. 1-8, 2010.

[107] S. Alok, S. K. Jain, A. Verma, M. Kumar, A. Mahor, and M. Sabharwal, "Plant profile, phytochemistry and pharmacology of Asparagus racemosus."

[108] B. Joseph and S. J. Raj, "An overview-Ficus bengalensis Linn," *International Journal of Pharmaceutical Sciences Review and Research,* vol. 6, pp. 21-24, 2011.

[109] S. Acharya, N. Acharya, J. Bhangale, S. Shah, and S. Pandya, "Antioxidant and hepatoprotective action of Asparagus racemosus Willd. root extracts," 2012.

[110] G. J. Darlington, S. E. Ross, and O. A. MacDougald, "The role of C/EBP genes in adipocyte differentiation," *Journal of Biological Chemistry,* vol. 273, pp. 30057-30060, 1998.

[111] A. Chawla, E. J. Schwarz, D. D. Dimaculangan, and M. A. Lazar, "Peroxisome proliferator-activated receptor (PPAR) gamma: adipose-predominant expression and induction early in adipocyte differentiation," *Endocrinology,* vol. 135, pp. 798-800, 1994.

[112] G. Medina-Gomez, S. Gray, and A. Vidal-Puig, "Adipogenesis and lipotoxicity: role of peroxisome proliferator-activated receptor γ (PPARγ) and PPARγcoactivator-1 (PGC1)," *Public health nutrition,* vol. 10, pp. 1132-1137, 2007.

[113] G. M. Morris, D. S. Goodsell, R. S. Halliday, R. Huey, W. E. Hart, R. K. Belew, and A. J. Olson, "Automated docking using a Lamarckian genetic algorithm and an empirical binding free energy function," *Journal of computational chemistry,* vol. 19, pp. 1639-1662, 1998.

[114] E. F. Pettersen, T. D. Goddard, C. C. Huang, G. S. Couch, D. M. Greenblatt, E. C. Meng, and T. E. Ferrin, "UCSF Chimera—a visualization system for exploratory research and analysis," *Journal of computational chemistry,* vol. 25, pp. 1605-1612, 2004.

[115] J. Kehrer, S. Biswal, P. THUILLIER, K. DATTA, S. FISCHER, and H. J. VANDEN, "Inhibition of peroxisome-proliferator-activated receptor (PPAR) α by MK886," *Biochem. J,* vol. 356, pp. 899-906, 2001.

[116] S. Hidalgo-Figueroa, J. J. Ramírez-Espinosa, S. Estrada-Soto, J. C. Almanza-Pérez, R. Román-Ramos, F. J. Alarcón-Aguilar, J. V. Hernández-Rosado, H. Moreno-Díaz, D. Díaz-Coutiño, and G. Navarrete-Vázquez, "Discovery of Thiazolidine-2, 4-Dione/Biphenylcarbonitrile Hybrid as Dual PPAR α/γ Modulator with Antidiabetic Effect: In vitro, In Silico and In Vivo Approaches," *Chemical biology & drug design,* 2013.

[117] N. Bopana and S. Saxena, "*Asparagus racemosus* - Ethnopharmacological evaluation and conservation needs," *Journal of Ethnopharmacology,* vol. 110, pp. 1-15, 2007.

[118] A. Sharma and V. Sharma, "A Brief Review Of Medicinal Properties Of *Asparagus racemosus* (Shatavari)," *International Journal Of Pure & Applied Biosciences,* vol. 1, pp. 48-52, 2013.

[119] A. K. Sachan, D. R. Das, S. L. Dohare, and M. Shuaib, "*Asparagus racemosus* (Shatavari): An Overview," *International Journal Of Pharmaceutical And Chemical Sciences,* vol. 1, pp. 588-592, 2012.

[120] V. Ashajyothi, R. S. Pippalla, and S. D, "*Asparagus racemosus* - A Phytoestrogen," *International Journal Of Pharmacy & Technology,* vol. 1, pp. 36-47, 2009.

[121] M. Sharma, A. Sharma, and A. Kumar, "Ethnopharmacological Importance Of *Asparagus racemosus*: A Review," *Journal Of Pharmaceutical And Biomedical Sciences*, vol. 6, pp. 1-12, 2011.

[122] S. K. Mitra, N. S. Prakash, and R. Sundaram, "Shatavarins (containing Shatavarin IV) with anticancer activity from the roots of Asparagus racemosus," *Indian journal of pharmacology*, vol. 44, p. 732, 2012.

[123] T. Sekine, N. Fukusawa, Y. Kashiwagi, N. Ruangrungsi, and I. Murakoshi, "Structure of asparagamine A, novel polycyclic alkaloid from Asparagus racemosus," *Chemical and pharmaceutical bulletin*, vol. 42, pp. 1360-1362, 1994.

[124] T. Sekine, F. Ikegami, N. Fukasawa, Y. Kashiwagi, T. Aizawa, Y. Fujii, N. Ruangrungsi, and I. Murakoshi, "Structure and relative stereochemistry of a new polycyclic alkaloid, asparagamine A, showing anti-oxytocin activity, isolated from Asparagus racemosus," *J. Chem. Soc., Perkin Trans. 1*, pp. 391-393, 1995.

[125] S. Tip-Pyang, P. Tangpraprutgul, N. Wiboonpun, G. Veerachato, P. Phuwapraisirisan, and B. Sup-Udompol, "Asparagamine A, an in vivo anti-oxytocin and antitumor alkaloid from Asparagus racemosus," *ACGC Chemical Research Communications*, vol. 12, pp. 31-35, 2000.

[126] N. Wiboonpun, P. Phuwapraisirisan, and S. Tip pyang, "Identification of antioxidant compound from Asparagus racemosus," *Phytotherapy Research*, vol. 18, pp. 771-773, 2004.

[127] D. Banerjee and R. Bhattacharyya, "Isoniazid and thioacetazone may exhibit antitubercular activity by binding directly with the active site of mycolic acid cyclopropane synthase: Hypothesis based on computational analysis," *Bioinformation*, vol. 8, p. 787, 2012.

[128] K. E. Lougheed, S. A. Osborne, B. Saxty, D. Whalley, T. Chapman, N. Bouloc, J. Chugh, T. J. Nott, D. Patel, and V. L. Spivey, "Effective inhibitors of the essential kinase PknB and their potential as anti-mycobacterial agents," *Tuberculosis*, vol. 91, pp. 277-286, 2011.

[129] C. Marzolini, A. Telenti, T. Buclin, J. Biollaz, and L. A. Decosterd, "Simultaneous determination of the HIV protease inhibitors indinavir, amprenavir, saquinavir, ritonavir, nelfinavir and the non-nucleoside reverse transcriptase inhibitor efavirenz by high-

performance liquid chromatography after solid-phase extraction," *Journal of Chromatography B: Biomedical Sciences and Applications,* vol. 740, pp. 43-58, 2000.

[130] D. Spinks, E. J. Shanks, L. A. Cleghorn, S. McElroy, D. Jones, D. James, A. H. Fairlamb, J. A. Frearson, P. G. Wyatt, and I. H. Gilbert, "Investigation of trypanothione reductase as a drug target in Trypanosoma brucei," *ChemMedChem,* vol. 4, pp. 2060-2069, 2009.

[131] J. T. Nguyen, Y. Hamada, T. Kimura, and Y. Kiso, "Design of potent aspartic protease inhibitors to treat various diseases," *Archiv der Pharmazie,* vol. 341, pp. 523-535, 2008.

[132] A. Gil L, P. A. Valiente, P. G. Pascutti, and T. Pons, "Computational Perspectives into Plasmepsins Structure—Function Relationship: Implications to Inhibitors Design," *Journal of tropical medicine,* vol. 2011, pp. 1-15, 2011.

[133] A. Brik and C.-H. Wong, "HIV-1 protease: mechanism and drug discovery," *Organic & biomolecular chemistry,* vol. 1, pp. 5-14, 2003.

[134] C. N. Deivanayagam, S. Rajasekaran, R. Venkatesan, A. Mahilmaran, P. Ahmed, S. Annadurai, S. Kumar, C. Chandrasekar, N. Ravichandran, and R. Pencillaiah, "Prevalence of acquired MDR-TB and HIV co-infection," *Indian Journal of Chest Diseases and Allied Sciences,* vol. 44, pp. 237-242, 2002.

[135] S. Sharma, A. Mohan, and T. Kadhiravan, "HIV-TB co-infection: epidemiology, diagnosis & management," *Indian Journal of Medical Research,* vol. 121, pp. 550-567, 2005.

[136] M. S. Glickman, S. M. Cahill, and W. R. Jacobs, "The Mycobacterium tuberculosis cmaA2 gene encodes a mycolic acid trans-cyclopropane synthetase," *Journal of Biological Chemistry,* vol. 276, pp. 2228-2233, 2001.

[137] Y. Av-Gay, S. Jamil, and S. J. Drews, "Expression and characterization of the Mycobacterium tuberculosis serine/threonine protein kinase PknB," *Infection and immunity,* vol. 67, pp. 5676-5682, 1999.

[138] M. O. F. Khan, "Trypanothione reductase: a viable chemotherapeutic target for antitrypanosomal and antileishmanial drug design," *Drug target insights,* vol. 2, pp. 129-146, 2007.

[139] M. Brüggemann, A. I. McDonald, L. E. Overman, M. D. Rosen, L. Schwink, and J. P. Scott, "Total synthesis of (±)-didehydrostemofoline (asparagamine A) and (±)-

isodidehydrostemofoline," *Journal of the American Chemical Society,* vol. 125, pp. 15284-15285, 2003.

[140] J. Lu, S. K. Vodnala, A.-L. Gustavsson, T. N. Gustafsson, B. Sjöberg, H. A. Johansson, S. Kumar, A. Tjernberg, L. Engman, and M. E. Rottenberg, "Ebsulfur is a benzisothiazolone cytocidal inhibitor targeting the trypanothione reductase of Trypanosoma brucei," *Journal of Biological Chemistry,* vol. 288, pp. 27456-27468, 2013.

[141] G. F. Pierce, "Inflammation in nonhealing diabetic wounds: the space-time continuum does matter," *The American journal of pathology,* vol. 159, p. 399, 2001.

[142] Q. Mi, B. Rivière, G. Clermont, D. L. Steed, and Y. Vodovotz, "Agent-based model of inflammation and wound healing: insights into diabetic foot ulcer pathology and the role of transforming growth factor-β1," *Wound Repair and Regeneration,* vol. 15, pp. 671-682, 2007.

[143] E. Shacter and S. A. Weitzman, "Chronic inflammation and cancer," *Oncology,* vol. 16, pp. 217-230, 2002.

[144] L. M. Coussens and Z. Werb, "Inflammation and cancer," *Nature,* vol. 420, pp. 860-867, 2002.

[145] V. P. Menon and A. R. Sudheer, "Antioxidant and anti-inflammatory properties of curcumin," in *The Molecular Targets and Therapeutic Uses of Curcumin in Health and Disease*, ed: Springer, 2007, pp. 105-125.

[146] A. Murakami and H. Ohigashi, "Targeting NOX, INOS and COX-2 in inflammatory cells: Chemoprevention using food phytochemicals," *International journal of cancer,* vol. 121, pp. 2357-2363, 2007.

[147] R. L. Thangapazham, A. Sharma, and R. K. Maheshwari, "Multiple molecular targets in cancer chemoprevention by curcumin," *The AAPS journal,* vol. 8, pp. E443-E449, 2006.

[148] B. B. Aggarwal, A. Kumar, and A. C. Bharti, "Anticancer potential of curcumin: preclinical and clinical studies," *Anticancer Res,* vol. 23, pp. 363-398, 2003.

[149] G. Bar-Sela, R. Epelbaum, and M. Schaffer, "Curcumin as an anti-cancer agent: review of the gap between basic and clinical applications," *Current medicinal chemistry,* vol. 17, pp. 190-197, 2010.

[150] T. Silambarasi, S. Latha, M. Thambidurai, and P. Selvamani, "FORMULATION AND EVALUATION OF CURCUMIN LOADED MAGNETIC NANOPARTICLES FOR

CANCER THERAPY," *International Journal of Pharmaceutical Sciences & Research*, vol. 3, 2012.